



Modelling acid gas mixtures of polar aprotic solvents and CO₂ with the Cubic Plus Association equation of state

Follegatti-Romero, Luis A.; Oller do Nascimento, Cláudio A.; Liang, Xiaodong

Published in:
Journal of Supercritical Fluids

Link to article, DOI:
[10.1016/j.supflu.2020.105052](https://doi.org/10.1016/j.supflu.2020.105052)

Publication date:
2021

Document Version
Peer reviewed version

[Link back to DTU Orbit](#)

Citation (APA):
Follegatti-Romero, L. A., Oller do Nascimento, C. A., & Liang, X. (2021). Modelling acid gas mixtures of polar aprotic solvents and CO₂ with the Cubic Plus Association equation of state. *Journal of Supercritical Fluids*, 167, Article 105052. <https://doi.org/10.1016/j.supflu.2020.105052>

General rights

Copyright and moral rights for the publications made accessible in the public portal are retained by the authors and/or other copyright owners and it is a condition of accessing publications that users recognise and abide by the legal requirements associated with these rights.

- Users may download and print one copy of any publication from the public portal for the purpose of private study or research.
- You may not further distribute the material or use it for any profit-making activity or commercial gain
- You may freely distribute the URL identifying the publication in the public portal

If you believe that this document breaches copyright please contact us providing details, and we will remove access to the work immediately and investigate your claim.

Modelling Acid Gas Mixtures of Polar Aprotic Solvents and CO₂ with the Cubic Plus Association Equation of State

Luis A. Follegatti-Romero^{a*}; Cláudio A. Oller do Nascimento^a; Xiaodong Liang^b

^a Laboratory of Separation and Purification Engineering (LaSPE), Department of Chemical Engineering (PQI), Polytechnic School (EP), University of São Paulo (USP), São Paulo – SP, Brazil

^b Center for Energy Resources Engineering (CERE), Department of Chemical and Biochemical Engineering, Technical University of Denmark, DK-2800 Kgs. Lyngby, Denmark

* Corresponding author: follegatti@usp.br

ABSTRACT

The Cubic Plus Association (CPA) equation of state and the Soave–Redlich–Kwong (SRK) equation of state coupled to Mathias–Copeman and volume correction parameters were used to correlate the vapor pressures and densities of pure polar aprotic solvents (PAS). It is shown that the CPA model (with 2B scheme) performed better than CPA (with inert scheme), SRK and its modifications in all cases for vapor pressure and densities. The performance of two mixing rules, namely the van der Waals one–fluid (vdW1f) and the Huron–Vidal (HV) mixing rules, is evaluated for these models on correlating the bubble–point pressures of CO₂ + PAS mixtures. The CPA–HV model performs best at several temperatures, with the global average absolute deviations equal to 7.2% for CPA–HV, 8.1% for CPA–vdW1f and 8.7% for SRK–HV. No improvements were found in the performance of the CPA–vdW1f when the solvation between CO₂ and PAS was accounted for regression of bubble–point pressures.

Keywords: CPA, SRK, polar aprotic solvents, CO₂, bubble–point pressures.

1. Introduction

The carbon capture and storage (CCS) concepts are abatement strategies for reducing anthropogenic carbon dioxide (CO₂) emissions, related with the greenhouse warming effect, that comprises separation of CO₂ from power plant flue gases, compression and transportation for geological storage in saline aquifers and reinjection of acid gases (hydrogen sulfide and CO₂) in deep reservoirs for enhanced oil recovery [1]. The large quantities of CO₂ and H₂S in expanding reserves of natural gas (more than 30% of the available gas fields are acid) defy the progress of gas separation technologies using physical absorption [2].

The mature carbon capture technologies for the removal of CO₂ are the post-combustion from fossil fuel power plants (CO₂ and N₂ separation) and natural gas sweetening from petroleum industry (CO₂ and H₂S separation), however, these individual process could increase the energy requirements of a plant by 25–40% [3,4]. Regarding the gas processing, the acid gases are generally removed from natural gas/gas streams by absorption/stripping process based in aqueous amine scrubbing (gas sweetening) solutions (typically between 15 to 60%), however its application in achieving zero emission is still not optimal, being necessary the integration of co-combustion of biomass to be economically viable [5,6]. Aqueous alkanolamine solutions are frequently used as solvent and present some disadvantages like a high corrosion rate (high concentrations), contamination of the outlet purified gas due to the high-water amount, high energy demand for amine regeneration process and high evaporation losses [6]. Therefore, technical challenges for separation technologies regarding to absorbents and solvents that perform the acid gas removal is essential to improve the design and optimization of gas treating process [7].

Recently, some polar aprotic solvents (PAS), like dimethyl sulfoxide (DMSO) and *N*-methyl-2-pyrrolidone (NMP), have been investigated for capturing CO₂ due to the fact that they can easily solubilize chemicals and pharmaceutical solutes, they are stable at elevated temperatures, water-soluble, low toxic, and they have high vapor pressure, reasonable price and negligible environmental impact [6,8]. The DMSO was reported as a solvent for ionic liquids for recovering CO₂ from industrial flue gas [8] and the NMP with the amine 2-amino-2-methyl-1-propanol in mixture was indicated by Karlsson et. al [9] for use in biogas purification and CCS. Other commercial PAS with high potential for CO₂ absorption, due to its low viscosities (essential to mass transfer) are acetonitrile (ACN), acetone, tetrahydrofuran (THF), methyl-ethyl ketone (MEK), *N, N*-dimethylformamide (DMF) and dichloromethane (DCM). Rochelle et al. [10] reported that the utilization of solvents instead of water in amine solutions could reduce the energy consumption to 0.2 megawatt-hour per ton of CO₂ due to the higher solubility of CO₂ in organic solvents and easy recovery of the solvent during the regeneration step of alkanolamines. Therefore, new requirements in the CO₂ removal by solvents, have been renewed and extended the necessity to obtain vapor-liquid equilibrium (VLE) data for CO₂ and proper solvent mixtures to improve the design of gas treatment processes which are essential for refining and reinjecting acid gases in geological formation to reduce CO₂ emissions.

Experimental thermodynamic data of the solubility of CO₂ in PAS over wide ranges of temperature and pressure have been published in the literature and the solubility data were correlated with several thermodynamic models. For example, the Peng-Robinson (PR) equation of state (EoS) was used for NMP,

ACN, THF, acetone, MEK and DMSO [11–13]; the Henry's constant or Gibbs energy correlated with a linear free energy relationship (LFER) analysis (for DMSO) [14], the extended Henry's law and Pitzer's virial expansion for the excess Gibbs energy and the Redlich–Kwong (RK) EoS (for DMSO and DMF) [15], the statistical associating fluid theory (SAFT) EoS for acetonitrile [16] and the quasi–chemical hydrogen–bonding (QCHB) model for dichloromethane (DCM) [17]. To the best of our knowledge, the Cubic Plus Association (CPA) EoS, has still not yet applied to correlate the experimental solubility data of binary mixtures of CO₂ and PAS except for acetone [18]. In order to design new installations and reach the best conditions in industrial scale, it is essential to improve the understanding of phase behavior of CO₂ and PAS mixtures and start with the thermodynamic modelling of phase behavior of CO₂ and suitable solvents [19].

The Soave–Redlich–Kwong (SRK) and the PR equations of state (EoS) are typically employed as primary choice models in petroleum industries, gas processing, etc. Nonetheless, these EoS do not provide accurate vapor pressure [20] and density [21] estimates at all conditions, attributed mainly to the limited amount of data available (critical properties and vapor pressures of heavy hydrocarbon compounds) for developing the original alpha function pertaining to both the SRK and PR EoS [22]. Thus, the Peneloux volume correction (1982) was developed to improve the predictions of the SRK EoS on liquid density up to 15% for hydrocarbon mixtures and up to 25% for water and methanol (polar compounds) [20,23]. Applying the constant volume translation (SRK–Peneloux), Lundstrøm et al. [20] achieved good results for liquid density data at 298.15 K and 373.15 with an error of 0.4% and 0.09%, respectively. When a constant volume translation is coupled to an EoS, the vapor pressure is unaffected [24], therefore, it requires an alpha correction, such as Mathias–Copeman coefficients to increase the accuracy of saturation pressure calculations [25].

It is common to use EoS in reservoir simulation with the classical mixing rule i.e. van der Waals one–fluid (vdW1f) mixing rule due to the ability for modeling phase equilibria for mixtures of hydrocarbons and the inorganic gases (CH₄, N₂, CO₂, etc.) at low– and high–pressure. However, some limitations as the poor modeling of VLE/liquid–liquid equilibria of mixtures in the presence of associating compounds and/or polar compounds have been reported [26,27]. Therefore, other mixing rules can be coupled to EoS aiming to avoid such limitations. For example, a successful mixing rule was formulated by Huron and Vidal (HV) [28] using the definition of the excess Gibbs energy from an EoS in 1979 [29]. Later still, Michelsen et al. [30] (1990) developed a modified Huron–Vidal (MHV) mixing rule for cubic EoS, incorporating directly parameters from existing G^E (for excess Gibbs energies) correlations, such as the nonrandom two–liquid (NRTL) model, for mixtures with more complex interactions. Pedersen et al. [31] applied satisfactorily the SRK–HV to predict the solubility of CH₄ in water.

The CPA EoS was developed in 1996 by Kontogeorgis et al. [32] which has been providing a practical and rigorous thermodynamic framework to model multicomponent mixtures relevant to oil and natural gas systems, e.g. those containing CO₂ with ethylene glycol (MEG), diethylene glycol (DEG) and triethylene glycol (TEG) [33], H₂S [34], water [35], alkanes [36], biofuels [37] and alcohols [38] using the classical van der Waals (CPA–vdW1f) mixing rule and covering a wide range of operation conditions from liquid to supercritical states. With the Huron–Vidal mixing rule, CPA (CPA–HV) has been applied to predict the phase equilibria for acetic acid,

water and other compounds [39]. Very recently, the CPA–HV was used by Xiong et al. [40] (2020) to predict satisfactorily the VLE of CH₄ and H₂O systems with a percentage average absolute deviation of 4.23% against 10.68% (CPA–vdW1f) and 20.86% (SRK–HV) for H₂O content in the CH₄–rich gas phase. Commonly, the SRK–HV is applied in modelling mixtures with acid gases, for example SRK with Huron–Vidal mixing rules obtained similar results to those calculated by CPA–vdW1f for CO₂–water–methane system using temperature–dependent binary interaction parameters [35,41]. On the other hand, Austegard et al. [41] (2006) reported that the CPA–EoS does not fit as well as the SRK–HV for the solubility of H₂O in liquid CO₂ and Pedersen et al. [42] (2001) used SRK–HV to predict the solubility of CO₂ in water with an absolute average percentage deviation of 5.2% using temperature dependent interaction parameters ranging from 288.15 to 548.15 K and 1–300 bar.

In this work, we have investigated the performance of the CPA EoS for correlating physical properties (vapor pressure and density) from the literature against the prediction of SRK EoS and its modifications (Mathias–Copeman coefficients and volume correction parameters), as well as the ability of the vdW1f and HV mixing rules coupled to CPA EoS in the description of VLE of CO₂ + PAS binary systems over a wide temperature and pressure ranges.

2. Thermodynamic models

2.1 The Cubic Plus Association (CPA EoS)

The CPA–EoS, proposed by Kontogeorgis et al. [32], combines the SRK EoS with an association term similar to that of SAFT,

$$Z = Z^{phys.} + Z^{assoc.} = \frac{1}{1 - b\rho} - \frac{a\rho}{RT(1 + b\rho)} - \frac{1}{2} \left(1 + \rho \frac{\partial \ln g}{\partial \rho} \right) \sum_i x_i \sum_{A_i} (1 - X_{A_i}) \quad (1)$$

where a is the energy parameter, b the co–volume parameter, ρ is the molar density, g a simplified hard–sphere radial distribution function, X_{A_i} the mole fraction of pure component i not bonded at site A , and x_i is the mole fraction of component i . The pure component energy parameter of Eq. (2), a , is obtained from a Soave–type temperature dependency:

$$a(T) = a_0 \left[1 + c_1 (1 - \sqrt{T_r}) \right]^2 \quad (2)$$

where a_0 and c_1 are often regressed (simultaneously with b) from pure component vapor pressure and liquid density data. X_{A_i} is related to the association strength $\Delta^{A_i B_j}$ between sites belonging to two different molecules and is calculated by solving the following set of equations:

$$X_{A_i} = \frac{1}{1 + \rho \sum_j x_j \sum_{B_j} X_{B_j} \Delta^{A_i B_j}} \quad (3)$$

$$\text{where } \Delta^{A_i B_j} = g(\rho) \left[\exp \left(\frac{\varepsilon^{A_i B_j}}{RT} \right) - 1 \right] b_{ij} \beta^{A_i B_j} \quad (4)$$

where $\varepsilon^{A_i B_j}$ and $\beta^{A_i B_j}$ are the association energy and the association volume, respectively. The simplified radial distribution function, $g(r)$, is given by [43]:

$$g(\rho) = \frac{1}{1-1.9\eta} \quad \text{where} \quad \eta = \frac{1}{4}b\rho = \frac{b}{4V} \quad (5)$$

where ρ is the pure compound density.

The objective function for parameters estimation is presented in the following equation:

$$OF = \sum_i^n \left(\frac{P_i^{\text{exp}} - P_i^{\text{cal}}}{P_i^{\text{exp}}} \right)^2 + \sum_i^n \left(\frac{\rho_i^{\text{exp}} - \rho_i^{\text{cal}}}{\rho_i^{\text{exp}}} \right)^2 \quad (6)$$

For binary mixtures, the energy and co-volume parameters of the physical term of the CPA EoS are calculated employing the Huron–Vidal (HV) [28] and the conventional van der Waals one–fluid mixing rules:

$$a = \sum_i \sum_j x_i x_j a_{ij} \quad \text{where} \quad a_{ij} = \sqrt{a_i a_j} (1 - k_{ij}) \quad (7)$$

$$b = \sum_i \sum_j x_i x_j b_{ij} \quad \text{where} \quad b_{ij} = \frac{b_i + b_j}{2} (1 - l_{ij}) \quad (8)$$

where the binary interaction parameter, k_{ij} , is the only adjustable binary interaction parameter.

For the Huron–Vidal mixing rule proposed by Huron and Vidal, a parameter of the SRK EoS is:

$$\frac{a}{b} = \sum_i x_i \frac{a_i}{b_i} - \frac{R}{\ln 2} \sum_i x_i \frac{\sum_j x_j b_j \exp\left(-\alpha_{ij} \frac{G_{ij}}{T}\right) G_{ji}}{\sum_j x_j b_j \exp\left(-\alpha_{ij} \frac{G_{ij}}{T}\right)} \quad (9)$$

where the asymmetric matrix G is temperature dependent

$$G_{ij} = G_{ij}^0 \quad (10)$$

$$G_{ji} = G_{ji}^0 \quad (11)$$

An important advantage of the HV mixing rule is that by setting $\alpha_{ij} = \alpha_{ji} = 0$ and by choosing G_{ij} and G_{ji} appropriately the classical one–fluid mixing rule (vdW1f) with k_{ij} is recovered. More details about the NRTL developed by Renon and Prausnitz [29] can be found in the literature [44,45].

When the CPA EoS is extended for mixtures containing two associating compounds, combining rules for the association term are required. The CR–1 combining rule was used in order to estimate the cross–associating parameters:

$$\varepsilon^{A_i B_j} = \frac{\varepsilon^{A_i B_i} + \varepsilon^{A_j B_j}}{2} \quad (12)$$

$$\beta^{A_i B_j} = \sqrt{\beta^{A_i B_i} \beta^{A_j B_j}} \quad (13)$$

or alternatively, the so–called Elliott combining rule (ECR) [34]

$$\Delta^{A_i B_j} = \sqrt{\Delta^{A_i B_i} \Delta^{A_j B_j}} \quad (14)$$

Assuming solvation (cross–association between a non–self–associating fluid and a self–associating one) between CO₂ and PAS, the modified CR–1 (mCR–1) was used in some cases [38]:

$$\beta^{A_i B_j} = \text{fitted to the experimental data} \quad (15)$$

$$\varepsilon^{A_i B_j} = \frac{\varepsilon_{associating}}{2} \quad (16)$$

156 In order to evaluate the performance of different models or modeling approaches, the percentage average
 157 absolute deviations (% AAD) between experimental thermodynamic data and calculated value from the models
 158 were obtained by:

$$\% AAD(\Omega) = \frac{1}{n} \sum_{i=1}^n \left| \frac{\Omega^{cal}}{\Omega^{exp}} - 1 \right| \times 100 \quad (17)$$

159 where Ω and n are the corresponding property and the number of experimental data points, respectively.

160

161 2.2 The Soave–Redlich–Kwong (SRK) EoS and its Modifications

162 The SRK EoS was developed by Soave in 1972 [22], in which the attractive pressure term of the Redlich–
 163 Kwong EoS [46] was replaced with a temperature dependent term “ $a(T)$ ” for pure compound, to give:

$$P = \frac{RT}{V - b} - \frac{a(T)}{V(V + b)} \quad (18)$$

$$a(T) = a_c \cdot \alpha(T) \quad (19)$$

$$a_c = 0.42747 \frac{(RT_c)^2}{P_c} \quad (20)$$

$$\alpha(T) = [1 + m(1 - \sqrt{T_r})]^2 \quad (21)$$

$$m = 0.480 + 1.574\omega - 0.17\omega^2 \quad (22)$$

$$b = 0.08664 \frac{RT_c}{P_c} \quad (23)$$

164 In order to provide a better description of the vapor pressure of polar compounds, Mathias–Copeman (SRK–
 165 MC) [25] suggested to modify the temperature term $a(T)$ as:

$$\alpha(T) = [1 + C_1(1 - \sqrt{T_r}) + C_2(1 - \sqrt{T_r})^2 + C_3(1 - \sqrt{T_r})^3]^2 \quad (24)$$

166 where $\alpha(T)$ is the Mathias–Copeman temperature–dependent term, which is a function of reduced temperature
 167 $T_r = T/T_c$. These three parameters are fitted to the experimental data of vapor pressure.

168 A procedure for improving the volumetric predictions of the SRK EoS by introducing a volume correction
 169 parameter “ c ” into the equation was developed by Peneloux et al. [23]:

$$P = \frac{RT}{V - b} - \frac{a(T)}{V + c(V + b + 2c)} \quad (25)$$

$$V_{peneloux} = V_{SRK} - c \quad (26)$$

$$b_{peneloux} = b_{SRK} - c \quad (27)$$

170 where V_{SRK} and $V_{penoloux}$ are SRK and Peneloux molar volumes, respectively.

The c parameter is the volume translation (VT) that in the original article by Peneloux was assumed as a constant and temperature independent for lighter components. In this work, the c parameter was obtained by the mean difference between the experimental and the molar volumes from the SRK EoS in the temperature range of the experimental data, as follow:

$$c = \frac{1}{n} \sum_{i=1}^n |V - V_{exp}| \quad (28)$$

For binary mixtures, the SRK EoS was also coupled with the Huron–Vidal mixing rule as described above.

3. CPA pure fluid parameters for polar aprotic solvents

The CPA EoS needs three pure component parameters in the cubic term (a_0 , c_1 and b) for non-associating components (inert scheme), while for associating compounds, two additional parameters in the association term (ε and β) and an associating scheme according to the nomenclature of Huang and Radosz [47] are required before calculations. It is important to emphasize that although the CPA EoS reduces to the SRK model for non-associating fluids, the pure fluid parameters are usually obtained by fitting the model to experimental data, whereas the SRK EoS uses critical properties (T_c , P_c and ω) for thermodynamic calculations.

Different association schemes for CO₂ were used in the CPA model to correlate physical properties and predict phase equilibria of binary systems containing acid gases. Depending on the mixture under investigation, the molecule of CO₂ was treated either as a self-associating fluid (having two, three or four association sites, i.e., 2B, 3B and 4C, respectively) [33,34], a non-self-associating fluid (inert) or solvating, assuming cross association, with polar/hydrogen bonding molecules (water or alcohols) [48]. Satisfactory results were found in modeling VLE for CO₂–alcohol/water mixtures (CO₂ was modeled as inert fluid) [34], for CO₂–alcohols systems assuming solvation (with 1 associating site) [38] and for CO₂–alcohol/water/diethyl ether systems when a 4C or self-associating CO₂ molecule was assumed [18,48,49]. Therefore, in this work, CO₂ is considered either as 4C association scheme (two proton donors + two proton acceptors) due to the exceptional performance for pure properties and phase behavior in previous works or as inert association scheme mainly for a comparison purpose.

On one hand, PAS are a group of substances with very weak capacity of proton-donating, because of the lack of O–H or N–H bonds, which means that they essentially do not associate with themselves, that is, these nucleophiles are relatively “free” in solution [50]. On the other hand, PAS are actually complex molecules with polar functional groups (atom double bonded to an oxygen atom) which normally dominate the characteristics of the solvents [51]. Although the CPA EoS does not take the polar effects into account explicitly, Folas et. al [52] and von Solms et. al [53] used an alternative approach to predict/regress the phase equilibria of systems containing polar compounds by assuming that these solvents are “pseudo-associating” or self-associating molecule having two association sites (2B) as well as in case of acetone [18]. Therefore, in this work, acetone and all polar aprotic solvents are considered as pseudo-associating compounds described with 2B scheme and for comparison purposes, the inert scheme is also considered. The new CPA pure compound parameters of PAS

were fitted to the available vapor pressure and liquid density data taken from the National Institute of Standards and Technology Thermo Data Engine (NIST TDE) in Aspen Plus V9 [54] (Table 2).

The energy (a_0), co-volume (b) and c_1 parameters were plotted against the van der Waals volume (vdW) of the compounds as shown in Figure 1. As we can see, the trends of energy (a_0) and c_1 pure parameters of the CPA EoS can be described very well by a quadratic polynomial equation while the co-volume (b) parameter can be accurately described by a linear correlation. In prior studies, it was observed that there is a correlation between the CPA pure parameters and vdW of glycerides, organic acids, n-alkanes, n-alcohols, methyl esters, ethyl esters and propyl esters [55,56]. The CPA pure parameters were also illustrated regarding molar mass of PAS and a clear polynomial trend was observed for the energy parameter and c_1 while the co-volume parameter is described by a straight line, as can be seen in Figure 3S (Supplementary Material). In this way, these correlations can allow the prediction of the corresponding CPA parameters for polar aprotic solvents in cases of lack of experimental data.

Table 2

CPA parameters for pure CO₂ and Pure Polar Aprotic solvents

Solvents	T_c (K)	M (kg/mol)	vdW (cm ³ /mol)	scheme	a_0 (L ² .bar/mol ²)	b (L/mol)	c_1	β	ε (bar.L/mol)	References
CO ₂	304.20	44.01	19.70	Inert	3.507	0.0272	0.76	–	–	[34]
				4C	3.140	0.0284	0.69	0.0297	39.23	
ACN	545.41	41.05	28.37	Inert	12.640	0.046	0.63	–	–	This work
				2B	4.590	0.042	1.16	0.689	137.30	
DCM	507.96	84.93	34.71	Inert	11.170	0.052	0.79	–	–	This work
				2B	7.472	0.053	1.00	0.411	75.096	
Acetone	508.06	58.08	39.04	2B	7.875	0.059	0.99	0.289	111.73	[18]
				Inert	13.71	0.060	0.8002	–	–	This work
				2B	7.927	0.059	0.97	0.226	116.68	
DMSO	722.0	78.13	42.88	Inert	21.390	0.069	0.84	–	–	This work
				2B	11.154	0.065	0.91	0.104	220.35	
THF	540.13	72.11	44.62	Inert	15.480	0.068	0.80	–	–	This work
				2B	11.03	0.067	0.91	0.296	86.74	
DMF	596.6	73.10	46.81	Inert	18.260	0.069	1.05	–	–	This work
				2B	12.225	0.067	0.89	0.042	199.09	
MEK	536.45	72.11	49.27	Inert	17.710	0.076	0.86	–	–	This work
				2B	13.441	0.075	0.82	0.126	117.64	
NMP	721.74	99.11	60.39	Inert	28.397	0.087	0.88	–	–	This work
				2B	23.068	0.087	0.77	0.089	150.47	

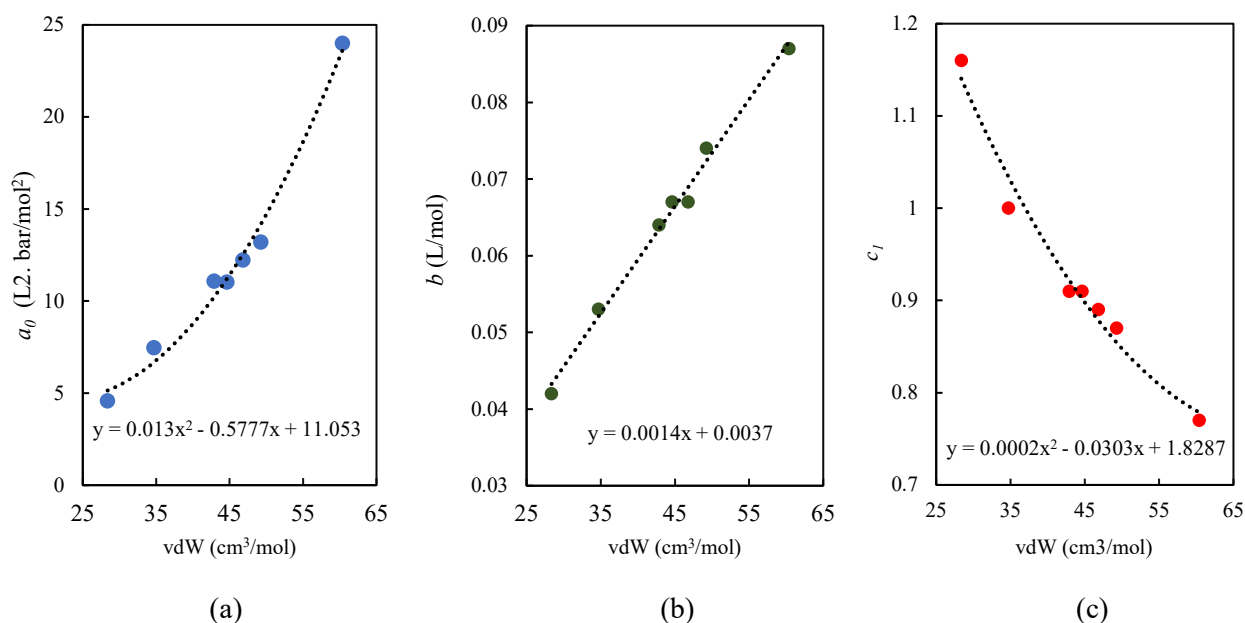


Figure 1. Variation of CPA parameters (2B) against van der Waals volume of Polar Aprotic Solvents: (a) energy “ a_0 ”, (b) co-volume “ b ” and (c) “ c_1 ”

4. Vapor Pressure and Density Calculations

The performance of the CPA EoS against the SRK EoS and its modifications in the calculation of vapor pressures and densities of polar aprotic solvents was evaluated over large temperature and pressure ranges. The polar aprotic solvents studied in this work are ACN, Acetone, THF, DMF, DMSO, MEK, DCM and NMP and they are modelled with the CPA EoS with two association schemes (inert and 2B), which were compared to the SRK EoS, the SRK EoS coupled to Mathias–Copeman (MC) and volume correction (VC) as well as the Antoine equation (only for vapor pressure).

Tables 1.1S and 1.3S (Supplementary Material) summarize the average absolute deviation (% AAD) and the overall average absolute deviation (% OAAD) of vapor pressures results for the polar aprotic solvents by using the SRK, SRK–MC–VC, Antoine Equation and CPA EoS. As expected, the SRK EoS, that is the original version, does not provide accurate predictions of vapor pressure and density for the studied polar aprotic solvents, as observed in Figure 2 (a and b) which depict the deviations between the experimental vapor pressures (from literature) and the modeling results with the equation of states. More precisely, the % OAAD were 10.6% for vapor pressures and 23.2% for densities, which clearly demonstrates the limitations of the SRK EoS with regard describing these properties of PAS and the necessity to apply the Mathias–Copeman and volume corrections, with which the deviation has been significantly reduced for vapor pressure (% OAAD = 1.25%) and liquid density (% OAAD = 0.72%). This values can be adequate if we consider the results reported in the literature, which indicate that deviations between 2 and 3% are considered satisfactory for liquid density for alkanes up to n–C29 taking into account the uncertainty of the experimental data [33].

Vapor pressures and densities were also calculated with the CPA EoS using 2B (5 adjustable parameters) and inert association schemes (3 adjustable parameters). The results for all PAS show that the CPA EoS presents

lower deviations as compared to the SRK EoS and its modifications. As presented in Tables 1.1S and 1.3S, the overall deviations (% *OAAD*) for bubble-points with 2B scheme and inert scheme were 0.5% and 0.68%, respectively. These deviations are lower than 1.0% obtained from the Antoine equation correlations for this property (parameters are listed in Table 1.2S). The results indicate that inert scheme gives very satisfactory description, while extra adjustable parameters by using 2B scheme give further improvement in the performance of the CPA to correlate vapor pressure of PAS, which are in very good agreement with previous studies [57], as shown in Fig. 2 (a). Very recently, Pourabadeh et. al. [58] (2020) reported the deviation of 4.63% for the bubble-points of NMP using the CPA EoS with inert scheme. In the case of densities, the % *OAAD* were 0.46% and 0.80% for 2B scheme and inert scheme, respectively. Again, the results demonstrate good performance of the CPA EoS (2B) on correlating experimental density data, as shown in Fig. 2 (b).

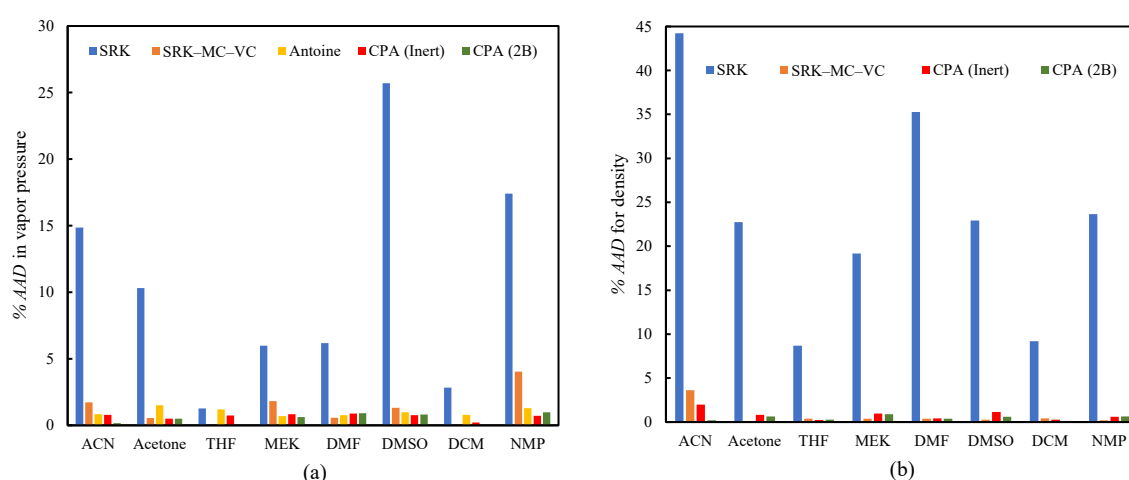


Figure 2. % AAD of models for vapor pressures (a) and densities (b) modeling

5. Modeling Bubble-Point Pressures of Polar Aprotic Solvent (PAS) + CO₂ Mixtures

In this work, the experimental bubble-point data from literature (58 isotherms) of binary systems containing PAS (ACN/Acetone/THF/MEK/DMF/DMSO/DCM/NMP) + CO₂ in a wide range of temperatures and pressures were modeled using CPA-vdW1f, CPA-HV and SRK-HV. In Table 1, eight different modeling approaches (cases) for the CPA EoS were considered for the PAS + CO₂ mixtures: inert-inert (case A), inert-4C (case B), 2B-inert (case C), and 4C-2B (case D), inert-inert (case E, HV), 4C-2B (case F, HV), 2B-solvation (case G). All approaches were compared against each other based on the overall deviations between the experimental data and modeling results and their accuracies were discussed and evaluated aiming to suggest the best modeling scenario. In such approaches, the PAS are treated either as being inert fluids or associating ones with two sites (2B), while CO₂ was modeled either as an inert compound (no associating sites), as a non-associating compound but with one proton-acceptor site for solvation or as a self-associating compound with four sites (4C).

As reported in the literature, the approaches 2B–inert (for acetone–hydrocarbon mixtures) [57] and solvation–4C (for acetone–CO₂ mixtures) [18,48,49] give satisfactory results. Therefore, it is important to point out that the concept of “pseudo–association” (able to act as associating compounds) which was adopted for PAS and CO₂ for accounting the polar interactions, with the intention to avoid explicit terms for the polar and/or quadrupolar interactions [18]. A single adjustable parameter for binary interactions (k_{ij}) was estimated for each binary system (cases A, B, C and D) for CPA–vdW1f by employing the combining rule CR–1 for the cross–association energy ($\varepsilon^{A_iB_j}$) and the cross–association volume ($\beta^{A_iB_j}$) of mixtures in the case of modeling two associating compounds. The best modeling approaches (A and D) from CPA–vdW1f were selected and the HV mixing rule coupled to the CPA EoS was applied in cases E and F. The HV mixing rule introduces two adjustable parameters (G_{ij}^0 and G_{ji}^0) with the non–randomness parameter (α_{ij}) fixed to 0.3. In case G (solvation case), the systems were modeled using eleven parameters, two adjustable parameters (the binary interaction parameter and the cross–association volume), one cross–association energy and eight pure parameters. Note that the case A utilizes less parameters than other cases (B, C, D, E, F and G modeling approaches), seven in total (6 pure and 1 binary parameters).

Table 1

Modelling approaches used with CPA for modelling bubble–points of PAS–CO₂ mixtures

Modelling approach	Association sites for PAS	Association sites for CO ₂	Cross–association parameters		Interaction parameters		Total parameters	
			$\beta^{A_iB_j}$	$\varepsilon^{A_iB_j}$	vdW1f (k_{ij})	HV(G_{ij}^0, G_{ji}^0)/ α_{ij}	Pure	Binary
Case A	Inert (no sites)	Inert (no sites)	–	–	Adjustable	–	6	1
Case B	Inert (no sites)	4C	CR–1	CR–1	Adjustable	–	8	3
Case C	2B	Inert (no sites)	CR–1	CR–1	Adjustable	–	8	3
Case D	2B	4C	CR–1	CR–1	Adjustable	–	10	3
Case E (HV)	Inert (no sites)	Inert (no sites)	–	–	–	Adjustable/Fixed	6	3
Case F (HV)	2B	4C	CR–1	CR–1	–	Adjustable/Fixed	10	5
Case G	2B	1 Negative site (solvation)	Adjustable	mCR–1	Adjustable	–	8	3

4C: two positive–two negative sites; 2B: one positive–one negative sites.

The parameters calculated/estimated and overall deviations of modeling approaches are presented in Tables 3 to 6. The binary interaction parameters obtained for CO₂ and PAS mixtures were either negative or positive values for A (inert–inert) and B (inert–4C) cases, as listed in Table 3 and illustrated in Figures 4.1S and 4.2S of the Supplementary Material. It is interesting to notice that the case C (2B–inert) presents small negative k_{ij} values, close to zero, whereas for the case D (2B–4C) all k_{ij} values were positives, as shown in Table 4. According Kontogeorgis and Folas [27], positive k_{ij} values are needed in by far most cases, whereas negative k_{ij} values are required for several solvating systems such as acetone–chloroform, acetone–methane or acetone–water due to that the cross–energy term is larger than the value provided by the geometric mean rule. Therefore, the negative binary interaction parameters estimated for cases A, B and C, although in almost all cases a good

representation of the bubble-points are obtained, suggest that the existing interactions must explicitly be taken into account, as in the case D. The trend of the binary interaction parameter was plotted against molar mass in Figures 4.1S to 4.4S. According to the correlations showed in that Figures, the binary interaction parameters slightly increase as the molecular weight of PAS increases for the cases A, B and C, while they are more or less constant for the case D. Similar behaviour (increasing k_{ij}) was observed with regard to the chain length of n-alkanes with N₂ using the CPA EoS [59] while the k_{ij} values decrease with chain length for heavier alkanes with CO₂, with regardless of it considered as either a self-associating or non-associating molecule with the CPA EoS [60]. However, some studies also showed that a constant trend of k_{ij} for asymmetric systems (CO₂-n-C₂₀ and CO₂-n-C₂₈) with the sPC-SAFT EoS [59], similar to what found in this work for the case D.

The performance of the CPA EoS coupled to the classical mixing rule (vdW1f) was evaluated in terms of their % *OAAD* and the results are listed in Tables 3 and 4. More details are available in Table 5S in Supplementary Materials. As presented in these tables, slightly better correlations ($k_{ij} \neq 0$) were obtained using the inert-inert (case A) and 4C-2B (case D) than cases B and C approaches for all binary systems at several pressures and temperatures. For example, the deviations for the ACN + CO₂ mixture, the cases A and D give 8.1% and 11.3%, respectively, while the cases B and C 11.9% and 15.3%, respectively. Particularly, in the case of MEK + CO₂ system, the cases A, B and C provided similar deviations 11.6%, 10.2% and 15.3%. In contrast, large deviations were found for the CO₂-DMSO mixture for the case B and C (69.7% and 39.4%, respectively). These results suggest that for modeling the CO₂ + PAS mixtures either inert-inert or 4C-2B schemes could be used with one binary interaction parameter fitted from the experimental VLE data. It is also worth highlighting that the inert-inert approach uses 6 CPA pure component parameters and 3 binary interaction parameters while the 4C-2B scheme uses 10 CPA pure component parameters and 3 binary interaction parameters. In both of them, a single adjustable parameter (k_{ij}) is employed.

The CPA-vdW1f results (cases A and D) were compared to those of CPA-HV (Cases E and F) and SRK-HV. It can be seen from the results (Tables 3 to 7) that, in terms of deviations (% *OAAD*), the CPA-HV model is slightly more accurate than the CPA-vdW1f and SRK-HV models, which two are comparable for modeling bubble-points for the ACN/Acetone/THF/MEK/DMF/DCM/NMP + CO₂ mixtures. For the THF-CO₂ mixture, the CPA-vdW1f model in cases A and D yield 2.7% and 2.6% overall absolute average deviations, respectively, while cases E, F and the SRK-HV model give 2.9%, 2.5% and 2.9%, respectively. These results are in agreement to those reported in the literature [40], in which the accuracy (less than 6.91%) of the CPA-HV model was better than the CPA-vdW1f and SRK-HV models for VLE of CH₄ + H₂O system. This can better be observed for DMSO + CO₂ mixture, where the case F (CPA-HV) showed an improved accuracy of 4.9%, whereas largest deviations were produced by the CPA-vdW1f (case A=10.1% and case D=12.9%) and SRK-HV (15.6%).

The global deviations are 7.2%, 8.1% and 8.7% for the CPA-HV, CPA-vdW1f (Cases A and D) and SRK-HV models, respectively. The improvement results obtained from the CPA-HV model with regard to the CPA-vdW1f model can be explained mainly due to the increase of number of adjustable parameters, whereas the

associative term from the CPA EoS provided an advantage in the regression of experimental data regarding the SRK–HV model. Therefore, the performance of the CPA EoS (both HV and vdW1f mixing rules) is very satisfactory in correlating the bubble–point pressures for CO₂ and polar aprotic solvents mixtures over extensive temperature ranges.

Figures 3 to 10 illustrate qualitatively the modeling approaches, which are concluded having better performance: CPA–vdW1f (2B–4C and Inert–Inert), CPA–HV (2B–4C and Inert–Inert), and SRK–HV, for the bubble–points calculations for the PAS + CO₂ binary systems over wide ranges of temperature and pressure. The four modeling approaches provide similarly satisfactory correlations/predictions of the bubble–points pressures for the ACN/Acetone/THF/DMF/MEK/DCM/NMP + CO₂ systems. Similar behavior was observed for the acetone–water binary where the results were improved by treating acetone as a self–associating molecule with the CPA EoS [18]. It is interesting to note that the SRK–HV model (using critical properties of pure substances and two adjustable parameters) shows worse deviations in predicting the bubble–point pressures as compared to the CPA EoS using CR–1 mixing rule for DMSO/NMP + CO₂ systems, as also seen in Fig. 8 and 10.

The “solvation” between CO₂ and PAS molecules was accounted for the case G (Table 7). For mixtures containing CO₂ and water/alcohols/glycols/ hydrocarbons, Tsvintzelis et al. [33] considered CO₂ as a non–self–associating fluid but one able to cross–associate with the self–associating fluids, good results were obtained when the mCR–1 was used to estimate the cross–association parameters. It is important to recall that the depending on its environment, CO₂ can act as proton acceptor forming hydrogen bonds [61]. Thus, although this treatment is helpful for mixtures containing water and glycols [52], the results of this work suggests that the “solvation” between CO₂ and PAS molecules does not help much to improve the performance of the CPA–vdW1f when the cross–association is accounted for regressing the bubble–points. For example, for CO₂ + ACN system, the two solvation methods (cases E and F) yield errors of 8.7% and 8.1%.

In summary, the CPA EoS is a good model for the CO₂–PAS mixtures by employing one or two adjustable parameters per binary system, i.e., using vdW1f or HV mixing rules. The difference of % *OAAD* between the cases A, D, E and F (four investigated modeling approaches) is marginal. Therefore, the case A (inert–inert) could be considered the best approach for modeling acid gas mixtures containing PAS and CO₂ as it uses the fewest number of adjustable parameters.

374 **Table 3**
 375 CPA–vdW1f Binary Interaction Parameters for acid Mixtures with PAS as Inert

Mixtures	Temperature range/K	Pressure range/bar	Case A (Inert–Inert)		Case B (Inert–4C)			
			k_{ij}	% <i>OAAD</i> ^a	k_{ij}	$\beta^{A_iB_j}$	$\varepsilon^{A_iB_j}$	% <i>OAAD</i> ^a
CO ₂ –ACN	298.00 – 348.20	0 – 120	–0.044	8.1	–0.140	172.34	235.93	11.9
CO ₂ –Acetone	291.15 – 353.18	0 – 120	–0.024	4.5	–0.091	172.34	235.93	4.5
CO ₂ –THF	298.00 – 353.20	0 – 110	–0.004	2.7	–0.068	172.34	235.93	2.8
CO ₂ –MEK	288.15 – 353.18	0 – 100	0.002	11.6	–0.064	172.34	235.93	10.2
CO ₂ –DMF	298.15 – 348.20	0 – 150	0.014	12.6	–0.057	172.34	235.93	13.6
CO ₂ –DMSO	298.15 – 348.15	0 – 180	–0.037	12.9	–0.004	172.34	235.93	59.7
CO ₂ –DCM	308.20 – 333.00	0 – 100	0.068	2.7	0.009	172.34	235.93	2.3
CO ₂ –NMP	243.10 – 398.15	0 – 320	–0.013	10.1	0.016	172.34	235.93	18.1

^a % Overall AAD = $\frac{1}{n} \sum_{n=1}^n$ % AAD, for bubble– points.

377
 378 **Table 4**
 379 CPA–vdW1f Binary Interaction Parameters for acid Mixtures with PAS as 2B

Mixtures	Temperature range/K	Case C (2B–Inert)				Case D (2B–4C)			
		k_{ij}	$\beta^{A_iB_j}$	$\varepsilon^{A_iB_j}/K$	% <i>OAAD</i> ^a	k_{ij}	$\beta^{A_iB_j}$	$\varepsilon^{A_iB_j}/K$	% <i>OAAD</i> ^a
CO ₂ –ACN	298.00 – 348.20	–0.119	830.1	825.7	15.3	0.059	0.143	1061.6	11.3
CO ₂ –Acetone	291.15 – 353.18	–0.129	475.3	701.8	9.5	0.028	0.082	937.7	4.3
CO ₂ –THF	298.00 – 353.20	–0.086	544.1	521.7	2.7	0.038	0.093	757.6	2.6
CO ₂ –MEK	288.15 – 353.18	–0.079	354.6	647.3	15.6	0.058	0.161	1426.6	10.2
CO ₂ –DMF	298.15 – 348.20	–0.025	204.8	1197.3	13.4	0.114	0.035	1433.3	12.6
CO ₂ –DMSO	298.15 – 348.15	–0.003	323.2	1325.2	39.4	0.096	0.058	1337.6	10.1
CO ₂ –DCM	308.20 – 333.00	–0.015	640.5	451.6	7.7	0.069	0.066	429.9	2.3
CO ₂ –NMP	243.10 – 398.15	–0.055	287.8	676.9	15.4	0.046	0.051	1141.9	11.4

^a % OAAD = $\frac{1}{n} \sum_{n=1}^n$ % AAD.

381
 382 **Table 5.**
 383 CPA–HV Interaction Parameters for CO₂ + Polar Aprotic Solvents Binary Systems

Mixtures	Case E (Inert–Inert)				Case F (2B–4C)			
	G_{ij}^o	G_{ji}^o	$\alpha_{ij} = \alpha_{ji}$	% <i>OAAD</i> ^a	G_{ij}^o	G_{ji}^o	$\alpha_{ij} = \alpha_{ji}$	% <i>OAAD</i> ^a
CO ₂ –ACN	–584.3	547.7	0.3	7.8	894.2	–195.5	0.3	7.7
CO ₂ –Acetone	41.8	–67.7	0.3	4.6	127.8	–7.06	0.3	4.3
CO ₂ –THF	12.88	12.78	538.2	2.9	–624.82	538.0	0.3	2.5
CO ₂ –MEK	–3.02	4.84	0.3	11.7	–81.76	142.9	0.3	9.9
CO ₂ –DMF	256.2	–19.01	0.3	12.4	680.1	42.86	0.3	11.9
CO ₂ –DMSO	–24.55	26.59	0.3	12.0	351.5	124.3	0.3	4.9
CO ₂ –DCM	–209.6	335.9	0.3	2.2	48.83	236.61	0.3	2.1
CO ₂ –NMP	–935.6	824.5	0.3	10.7	–935.67	824.52	0.3	8.6

^a % OAAD = $\frac{1}{n} \sum_{n=1}^n$ % AAD

389 **Table 6.**
 390 SRK–HV Interaction Parameters for CO₂ + Polar Aprotic Solvents Binary Systems

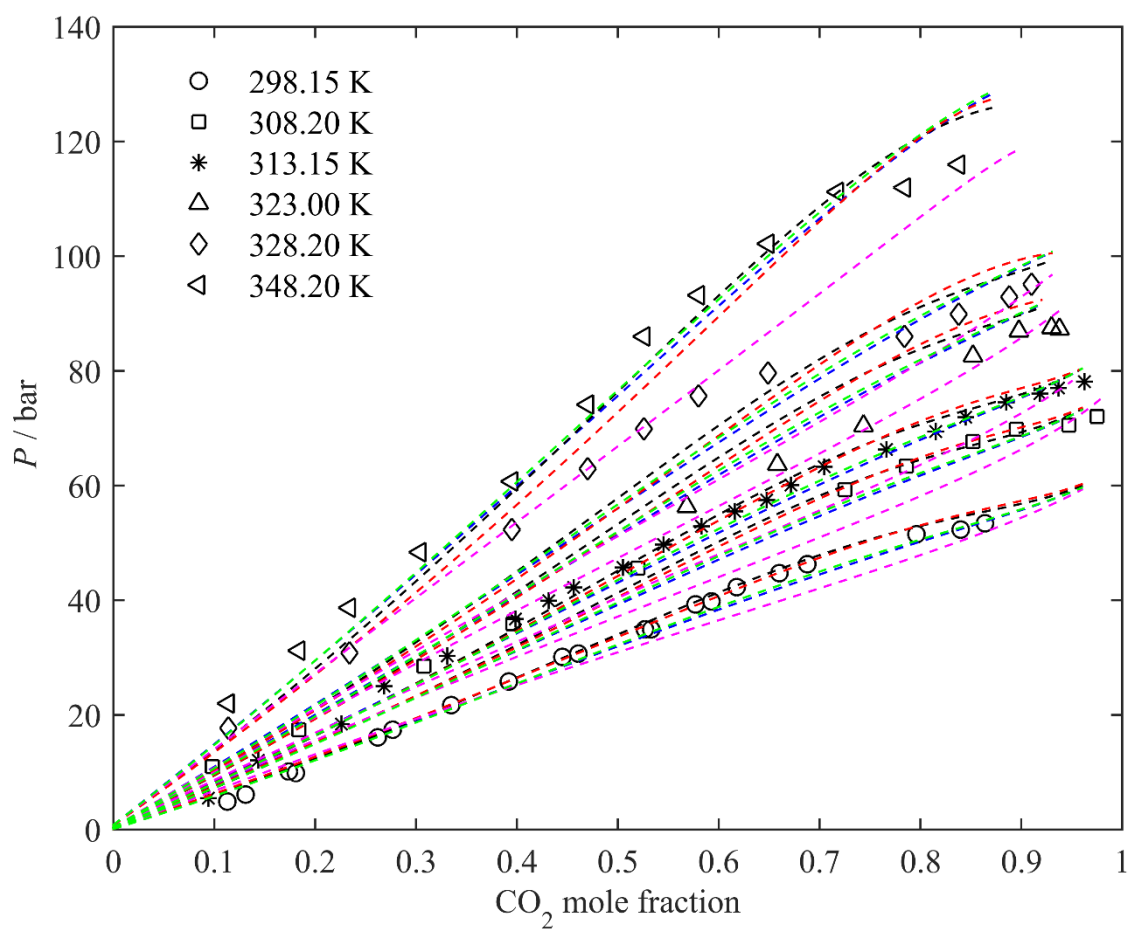
Mixtures	SRK–HV			
	G_{ij}^o	G_{ji}^o	$\alpha_{ij} = \alpha_{ji}$	% <i>OAAD</i> ^a
CO ₂ –ACN	643.02	−70.87	0.3	8.7
CO ₂ –Acetone	−1.10	−2.87	0.3	3.9
CO ₂ –THF	18.40	−18.05	0.3	2.9
CO ₂ –MEK	−31.84	45.76	0.3	10.6
CO ₂ –DMF	298.78	15.75	0.3	12.0
CO ₂ –DMSO	0.048	6.75	0.3	15.6
CO ₂ –DCM	68.82	133.51	0.3	3.1
CO ₂ –NMP	−345.18	154.66	0.3	11.2

391 ^a % *OAAD* = $\frac{1}{n} \sum_{n=1}^n$ % *AAD*.
 392

393 **Table 7**
 394 CPA–vdW1f Binary Interaction Parameters for acid Mixtures with Solvation of CO₂

Mixtures	Temperature range/ <i>K</i>	Case G			% <i>OAAD</i> ^a
		k_{ij}	$\beta^{A_iB_j}$	$\varepsilon^{A_iB_j}/K$	
CO ₂ –ACN	298.00 – 348.20	−0.017	824	825.6	8.7
CO ₂ –Acetone	291.15 – 353.18	0.024	858	701.7	5.3
CO ₂ –MEK	288.15 – 353.18	0.103	944	647.3	11.1
CO ₂ –DMF	298.15 – 348.20	0.064	196	1197.3	10.5
CO ₂ –DMSO	298.15 – 348.15	−0.285	1200	1325.2	45.8
CO ₂ –DCM	308.20 – 333.00	0.172	1640	451.6	3.6
CO ₂ –NMP	243.10 – 398.15	−0.013	122	676.9	12.5

395 ^a % *OAAD* = $\frac{1}{n} \sum_{n=1}^n$ % *AAD*.
 396



397

398 **Figure 3.** VLE experimental data of ACN-CO₂ (symbols) were taken from [16,62,63]. CPA-vdW1f: magenta
 399 lines (2B-4C) and blue lines (Inert-Inert). CPA-HV: black lines (2B-4C) and green lines (Inert-Inert). SRK-
 400 HV: red lines.

401

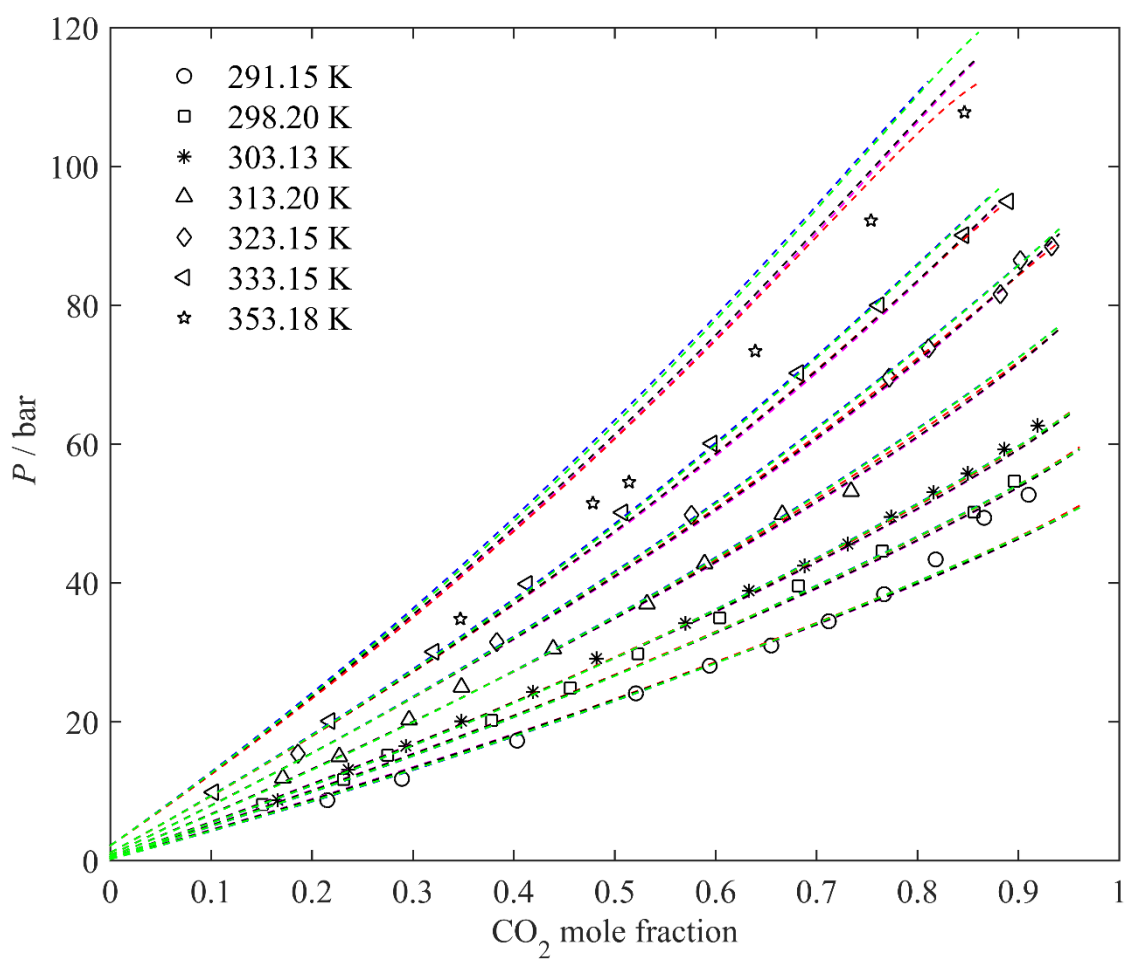


Figure 4. VLE experimental data of Acetone–CO₂ (symbols) were taken from [12,13,64–67]. CPA–vdW1f: magenta lines (2B–4C) and blue lines (Inert–Inert). CPA–HV: black lines (2B–4C) and green lines (Inert–Inert). SRK–HV: red lines.

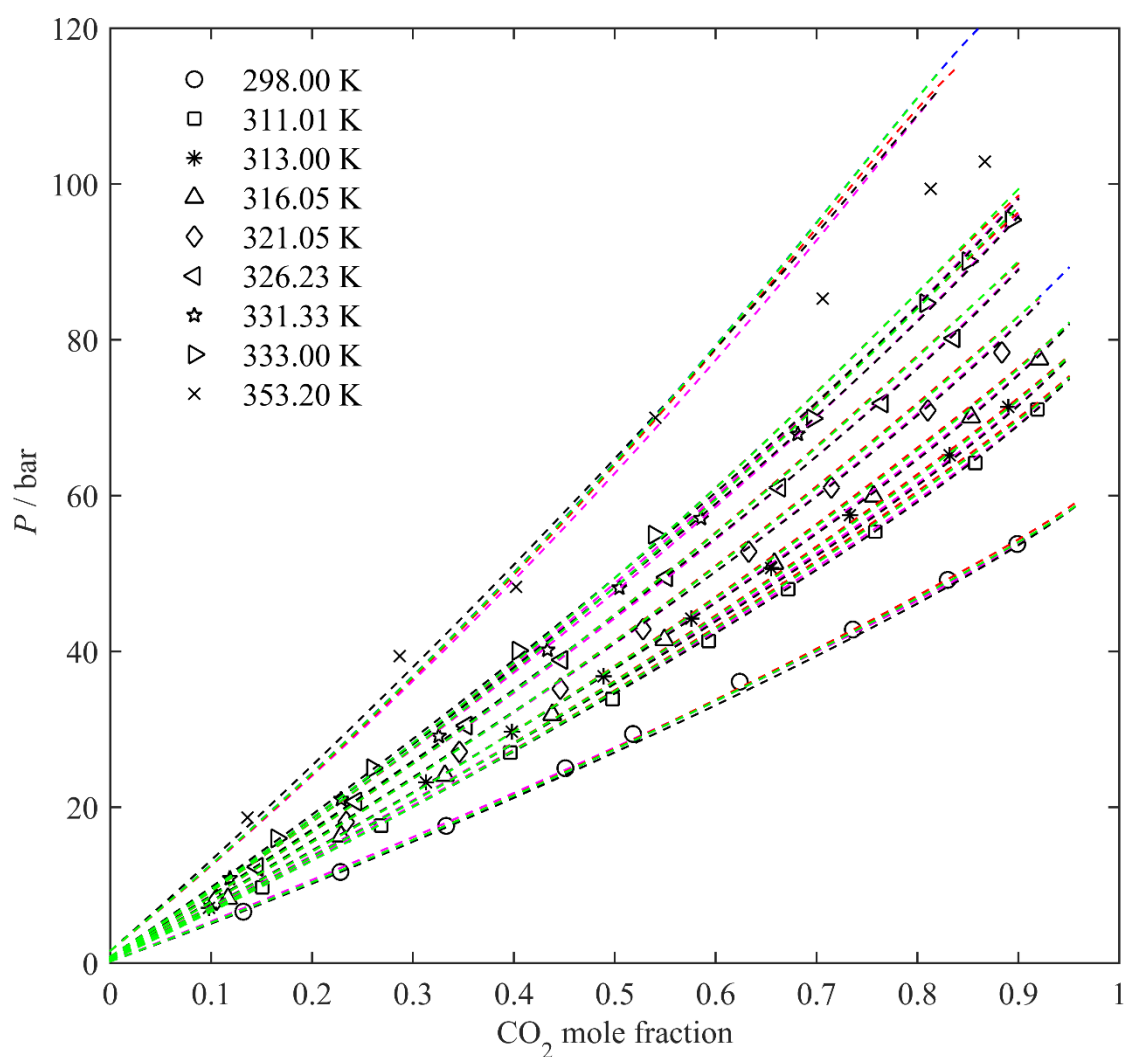


Figure 5. VLE experimental data of THF-CO₂ (symbols) were taken from [68–70]. CPA–vdW1f: magenta lines (2B–4C) and blue lines (Inert–Inert). CPA–HV: black lines (2B–4C) and green lines (Inert–Inert). SRK–HV: red lines.

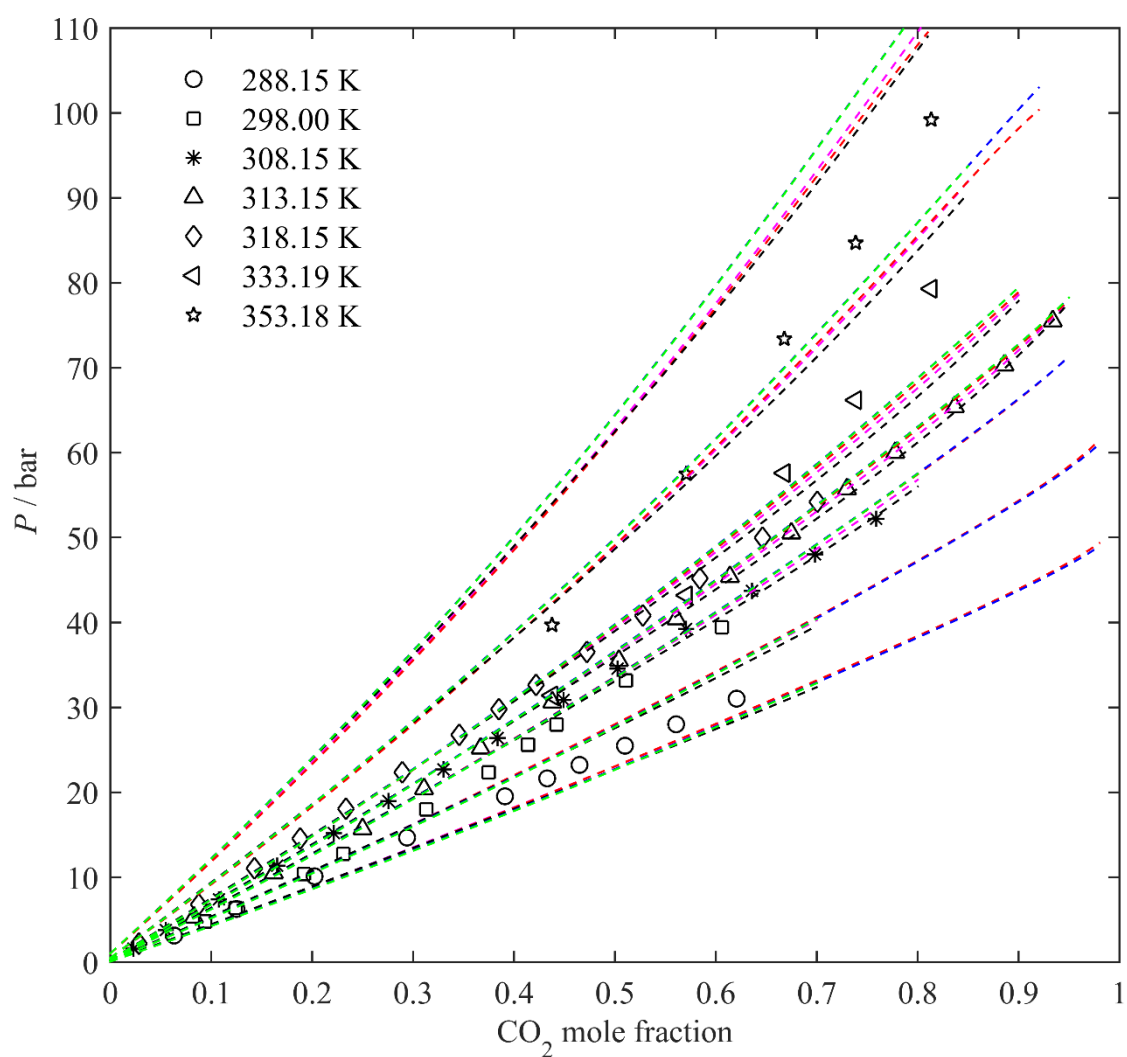


Figure 6. VLE experimental data of MEK–CO₂ (symbols) were taken from [13,71–73]. CPA–vdW1f: magenta lines (2B–4C) and blue lines (Inert–Inert). CPA–HV: black lines (2B–4C) and green lines (Inert–Inert). SRK–HV: red lines.

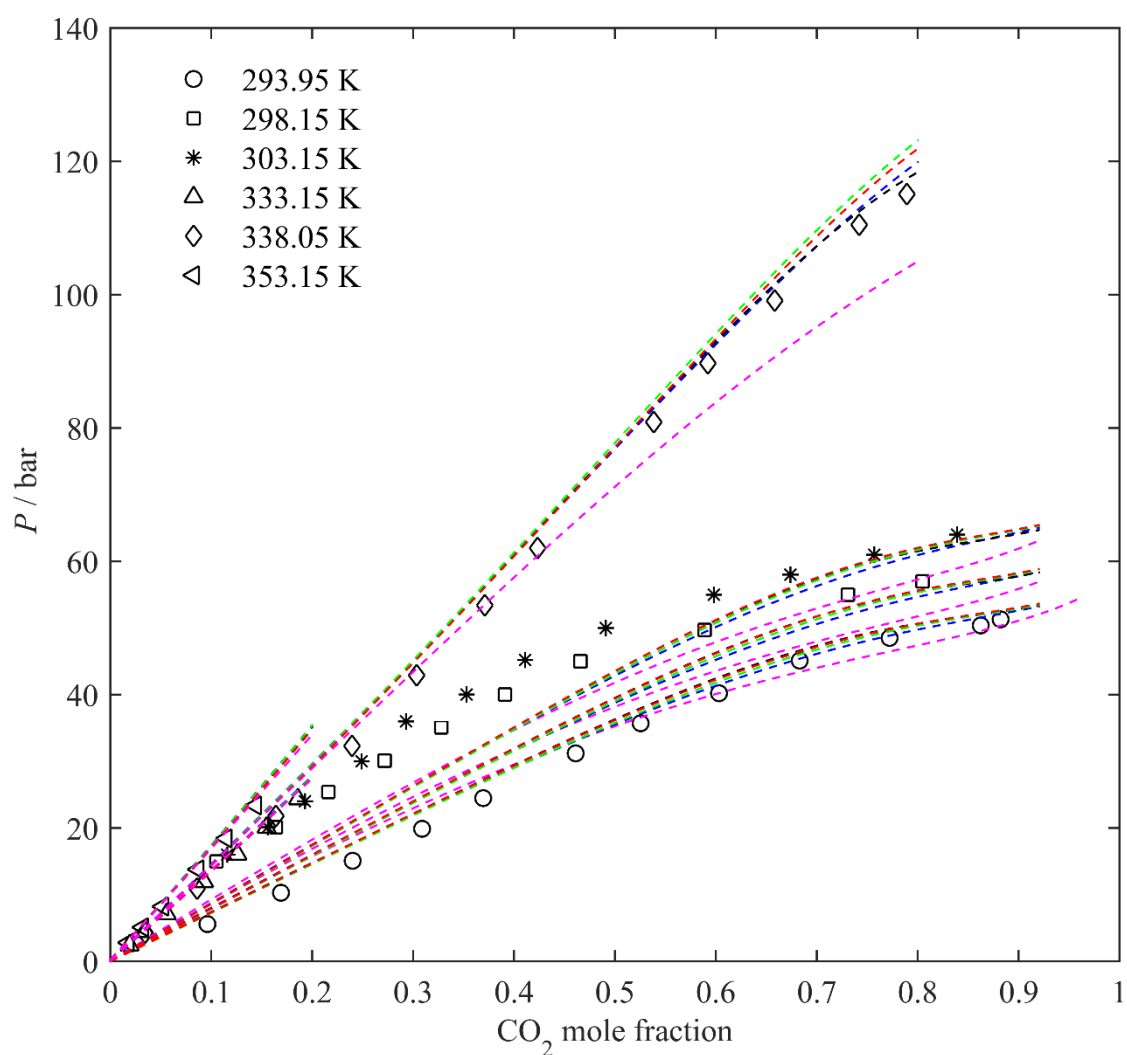


Figure 7. VLE experimental data of DMF-CO₂ (symbols) were taken from [15,62,74]. CPA-vdW1f: magenta lines (2B-4C) and blue lines (Inert-Inert). CPA-HV: black lines (2B-4C) and green lines (Inert-Inert). SRK-HV: red lines.

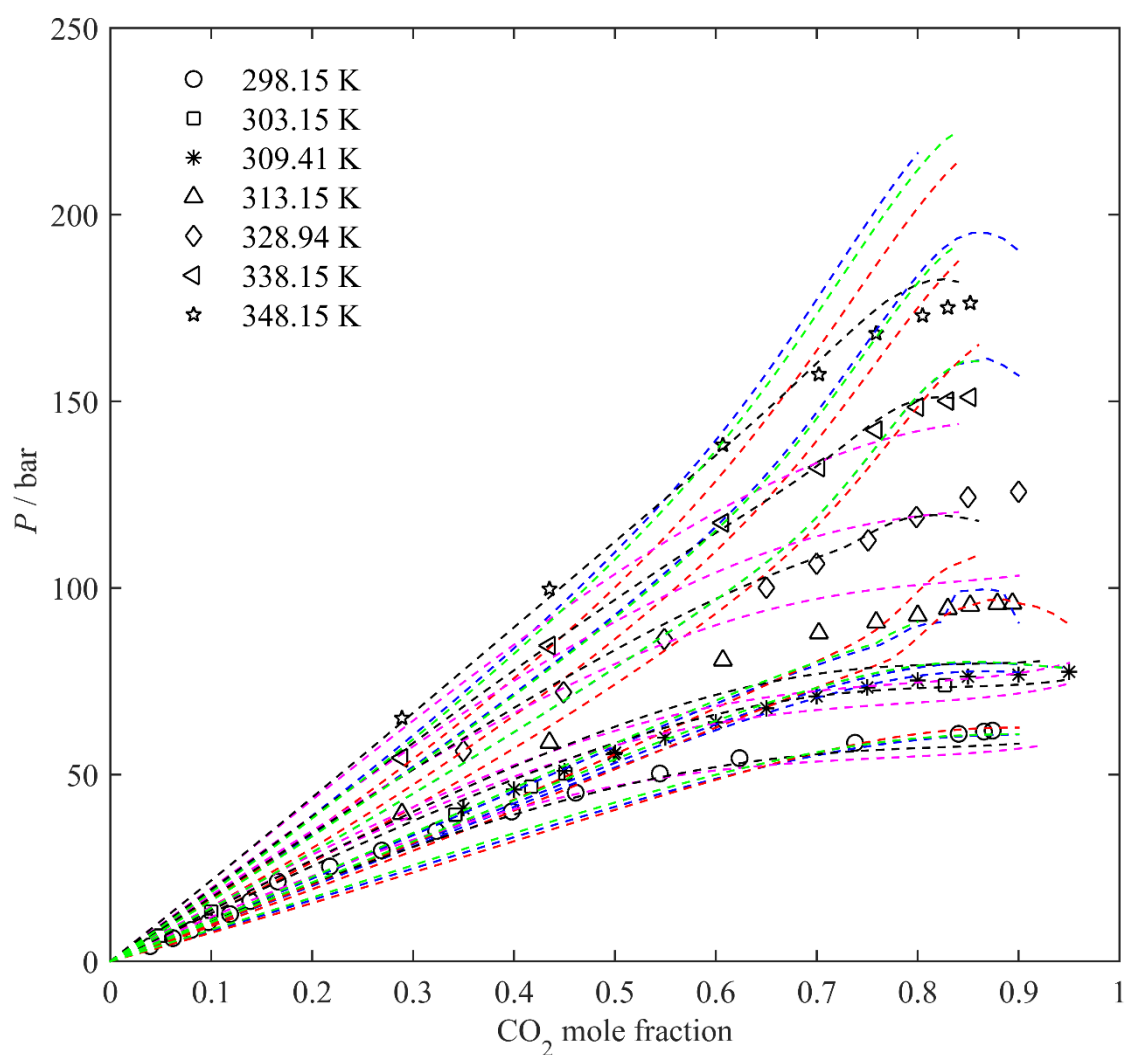


Figure 8. VLE experimental data of DMSO–CO₂ (symbols) were taken from [62,75,76]. CPA–vdW1f: magenta lines (2B–4C) and blue lines (Inert–Inert). CPA–HV: black lines (2B–4C) and green lines (Inert–Inert). SRK–HV: red lines.

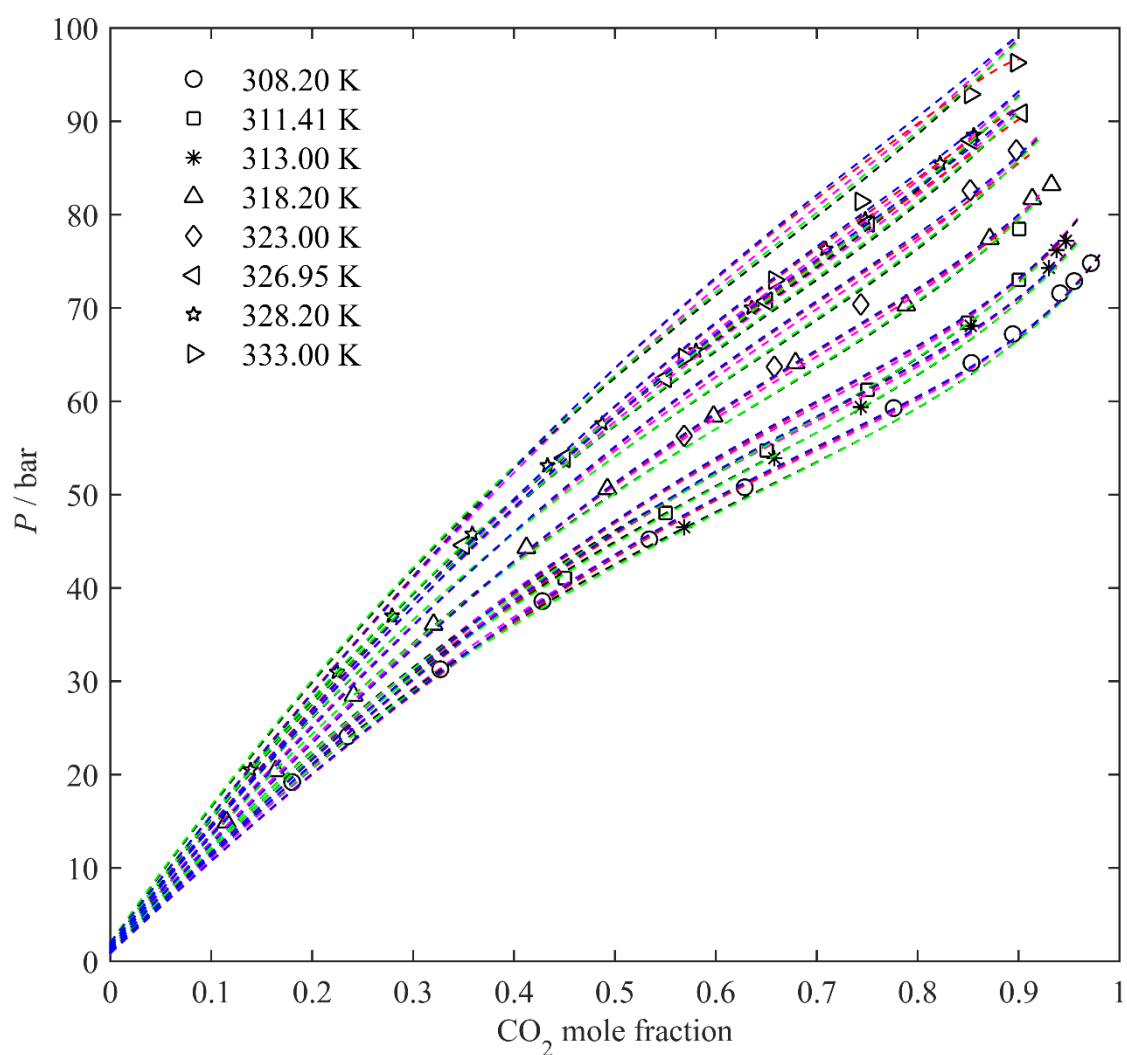


Figure 9. VLE experimental data of DCM-CO₂ (symbols) were taken from [17,63,76,77]. CPA-vdW1f: magenta lines (2B-4C) and blue lines (Inert-Inert). CPA-HV: black lines (2B-4C) and green lines (Inert-Inert). SRK-HV: red lines.

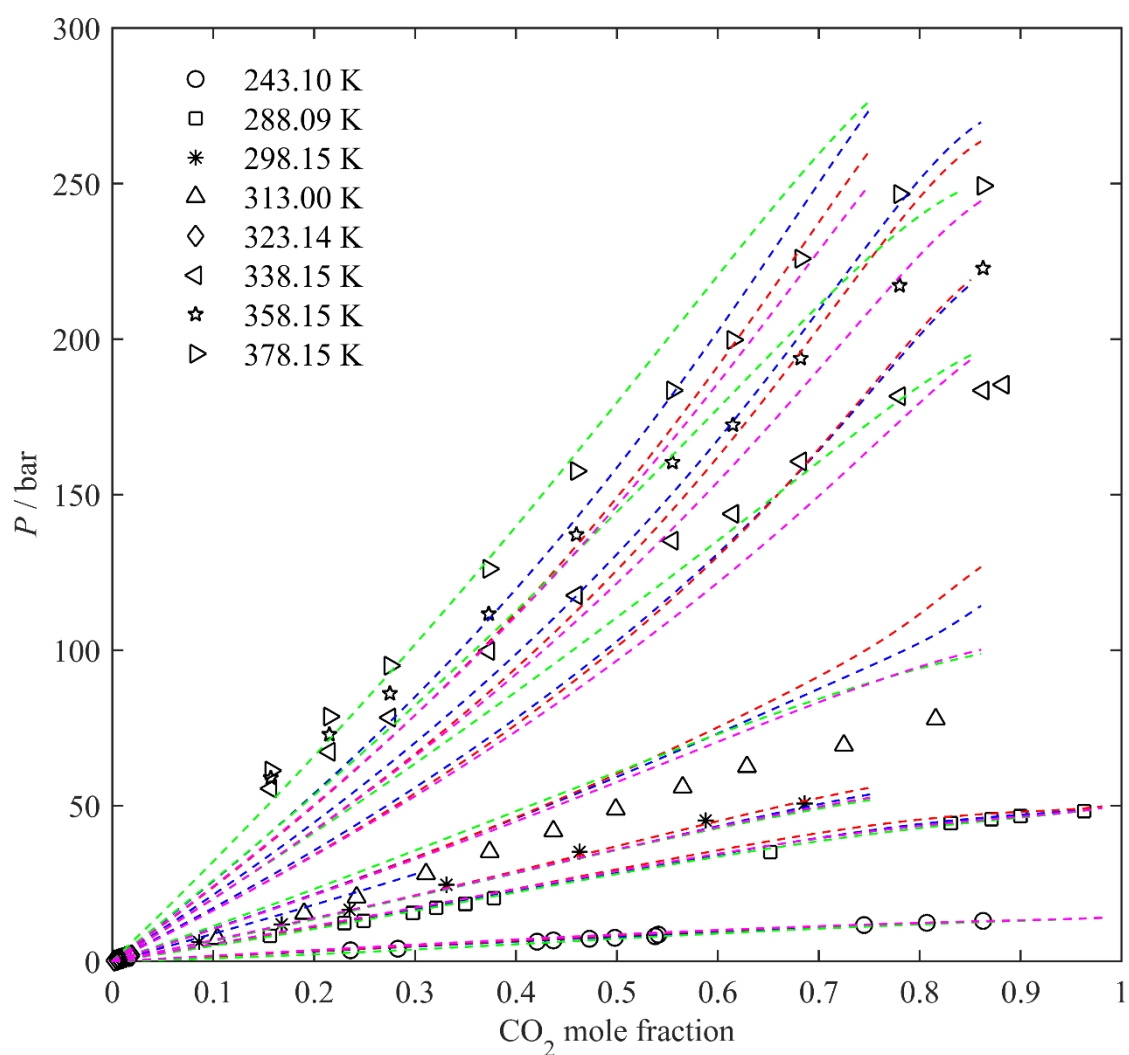


Figure 10. VLE experimental data of NMP-CO₂ (symbols) were taken from [78–80]. CPA–vdW1f: magenta lines (2B–4C) and blue lines (Inert–Inert). CPA–HV: black lines (2B–4C) and green lines (Inert–Inert). SRK–HV: red lines.

6. Conclusions

The CPA EoS was better than SRK and its modifications (Mathias–Copeman coefficients and volume correction parameters) in modeling vapor pressures and densities of polar aprotic solvents over extensive temperature and pressure ranges. The CPA–vdW1f provides goods results using 2B–4C and inert–inert association schemes for modeling bubble point pressures of PAS–CO₂ binary systems with a single adjustable binary interaction parameter and CR–1 combining rules for cross association parameters. The correlation of the bubble point pressures of relevant acid gas mixtures containing PAS + CO₂ employing the CPA coupled to Huron–Vidal (HV) mixing rules is slightly better than CPA coupled to van der Waals (vdW1f) and SRK–HV models. The associative term in CPA–HV improved the performance in comparison with SRK–HV. The solvation approach in the CPA–vdW1f does not improve the accuracy of model for PAS–CO₂ even employing one more adjustable parameter (case G). For all systems, such deviations are comparable to those calculated to the best approaches modeling (cases A and D). It was demonstrated that the CPA is a flexible thermodynamic tool for calculate accurately vapor pressure and density of pure PAS, as well as the bubble–point pressures of acid mixtures containing PAS and CO₂ available in the literature.

7. Acknowledgments

We gratefully acknowledge the support of the Research Center for Gas Innovation (RCGI), hosted by the University of São Paulo (USP) and sponsored by São Paulo Research Foundation (FAPESP – 2014/50279–4 and 2019/22085–4) and Shell Brazil. We are also grateful to professor Georgios M. Kontogeorgis for helpful suggestions.

8. Literature Cited

- [1] O. de Q.F. Araújo, J.L. de Medeiros, Carbon capture and storage technologies: present scenario and drivers of innovation, *Curr. Opin. Chem. Eng.* 17 (2017) 22–34. <https://doi.org/10.1016/J.COCHE.2017.05.004>.
- [2] I. Tsivintzelis, G.M. Kontogeorgis, M.L. Michelsen, E.H. Stenby, Modeling phase equilibria for acid gas mixtures using the CPA equation of state. I. Mixtures with H₂S, *AIChE J.* 56 (2010) 2965–2982. <https://doi.org/10.1002/aic.12207>.
- [3] D.M. D’Alessandro, B. Smit, J.R. Long, Carbon Dioxide Capture: Prospects for New Materials, *Angew. Chemie Int. Ed.* 49 (2010) 6058–6082. <https://doi.org/10.1002/anie.201000431>.
- [4] M. Wang, A.S. Joel, C. Ramshaw, D. Eimer, N.M. Musa, Process intensification for post-combustion CO₂ capture with chemical absorption: A critical review, *Appl. Energy.* 158 (2015) 275–291. <https://doi.org/10.1016/J.APENERGY.2015.08.083>.
- [5] K. Jiang, P.H.M. Feron, A. Cousins, R. Zhai, K. Li, Achieving zero/negative-emissions coal-fired power plants using amine-based post-combustion CO₂ capture technology and biomass co-combustion,

Environ. Sci. Technol. (2020). <https://doi.org/10.1021/acs.est.9b07388>.

[6] E. Davarpanah, S. Hernández, G. Latini, C.F. Pirri, S. Bocchini, Enhanced CO₂ Absorption in Organic Solutions of Biobased Ionic Liquids, *Adv. Sustain. Syst.* 4 (2020) 1900067. <https://doi.org/10.1002/adsu.201900067>.

[7] J. Gomes, S. Santos, J. Bordado, Choosing amine-based absorbents for CO₂ capture, *Environ. Technol.* 36 (2015) 19–25. <https://doi.org/10.1080/09593330.2014.934742>.

[8] H. Svensson, J. Edfeldt, V. Zejnullahu Velasco, C. Hultberg, H.T. Karlsson, Solubility of carbon dioxide in mixtures of 2-amino-2-methyl-1-propanol and organic solvents, *Int. J. Greenh. Gas Control.* 27 (2014) 247–254. <https://doi.org/10.1016/J.IJGGC.2014.06.004>.

[9] H.K. Karlsson, P. Drabo, H. Svensson, Precipitating non-aqueous amine systems for absorption of carbon dioxide using 2-amino-2-methyl-1-propanol, *Int. J. Greenh. Gas Control.* 88 (2019) 460–468. <https://doi.org/10.1016/J.IJGGC.2019.07.001>.

[10] G.T. Rochelle, Amine Scrubbing for CO₂ Capture, *Science* (80-.). 325 (2009) 1652 LP – 1654. <https://doi.org/10.1126/science.1176731>.

[11] R. Rajasingam, L. Lioe, Q.T. Pham, F.P. Lucien, Solubility of carbon dioxide in dimethylsulfoxide and N-methyl-2-pyrrolidone at elevated pressure, *J. Supercrit. Fluids.* 31 (2004) 227–234. <https://doi.org/10.1016/J.SUPFLU.2003.12.003>.

[12] Z. Lei, X. Qi, J. Zhu, Q. Li, B. Chen, Solubility of CO₂ in Acetone, 1-Butyl-3-methylimidazolium Tetrafluoroborate, and Their Mixtures, *J. Chem. Eng. Data.* 57 (2012) 3458–3466. <https://doi.org/10.1021/je300611q>.

[13] Y. Sato, N. Hosaka, K. Yamamoto, H. Inomata, Compact apparatus for rapid measurement of high-pressure phase equilibria of carbon dioxide expanded liquids, *Fluid Phase Equilib.* 296 (2010) 25–29. <https://doi.org/10.1016/J.FLUID.2009.12.030>.

[14] A.R. Harifi-Mood, Solubility of carbon dioxide in binary mixtures of dimethyl sulfoxide and ethylene glycol: LFER analysis, *J. Chem. Thermodyn.* 141 (2020) 105968. <https://doi.org/10.1016/J.JCT.2019.105968>.

[15] M. Shokouhi, H. Farahani, M. Hosseini-Jenab, Experimental solubility of hydrogen sulfide and carbon dioxide in dimethylformamide and dimethylsulfoxide, *Fluid Phase Equilib.* 367 (2014) 29–37. <https://doi.org/10.1016/J.FLUID.2014.01.020>.

[16] H.-S. Byun, B.M. Hasch, M.A. McHugh, Phase behavior and modeling of the systems CO₂-acetonitrile and CO₂-acrylic acid, *Fluid Phase Equilib.* 115 (1996) 179–192. [https://doi.org/10.1016/0378-3812\(95\)02830-7](https://doi.org/10.1016/0378-3812(95)02830-7).

[17] I. Tsivintzelis, D. Missopolinou, K. Kalogiannis, C. Panayiotou, Phase compositions and saturated densities for the binary systems of carbon dioxide with ethanol and dichloromethane, *Fluid Phase Equilib.* 224 (2004) 89–96. <https://doi.org/10.1016/J.FLUID.2004.06.046>.

[18] E. Voutsas, C. Perakis, G. Pappa, D. Tassios, An evaluation of the performance of the Cubic-Plus-Association equation of state in mixtures of non-polar, polar and associating compounds: Towards a

- single model for non-polymeric systems, *Fluid Phase Equilib.* 261 (2007) 343–350.
<https://doi.org/10.1016/J.FLUID.2007.07.051>.
- [19] H.A. Shirazizadeh, A. Haghtalab, Simultaneous solubility measurement of (ethyl mercaptan + carbon dioxide) into the aqueous solutions of (N-methyl diethanolamine + sulfolane + water), *J. Chem. Thermodyn.* 133 (2019) 111–122. <https://doi.org/10.1016/J.JCT.2019.02.003>.
- [20] C. Lundstrøm, M.L. Michelsen, G.M. Kontogeorgis, K.S. Pedersen, H. Sørensen, Comparison of the SRK and CPA equations of state for physical properties of water and methanol, *Fluid Phase Equilib.* 247 (2006) 149–157. <https://doi.org/10.1016/J.FLUID.2006.06.012>.
- [21] J.M. Prausnitz, F.W. Tavares, Thermodynamics of Fluid-Phase Equilibria for Standard Chemical Engineering Operations, *AIChE J.* 50 (2004) 739–761. <https://doi.org/10.1002/aic.10069>.
- [22] G. Soave, Equilibrium constants from a modified Redlich-Kwong equation of state, *Chem. Eng. Sci.* 27 (1972) 1197–1203. [https://doi.org/10.1016/0009-2509\(72\)80096-4](https://doi.org/10.1016/0009-2509(72)80096-4).
- [23] A. Péneloux, E. Rauzy, R. Fréze, A consistent correction for Redlich-Kwong-Soave volumes, *Fluid Phase Equilib.* 8 (1982) 7–23. [https://doi.org/10.1016/0378-3812\(82\)80002-2](https://doi.org/10.1016/0378-3812(82)80002-2).
- [24] K. Frey, M. Modell, J.W. Tester, Density-and-temperature-dependent volume translation for the SRK EOS: 2. Mixtures, *Fluid Phase Equilib.* 343 (2013) 13–23. <https://doi.org/10.1016/J.FLUID.2013.01.006>.
- [25] P.M. Mathias, T.W. Copeman, Extension of the Peng-Robinson equation of state to complex mixtures: Evaluation of the various forms of the local composition concept, *Fluid Phase Equilib.* 13 (1983) 91–108. [https://doi.org/10.1016/0378-3812\(83\)80084-3](https://doi.org/10.1016/0378-3812(83)80084-3).
- [26] D. Paterson, *Flash Computation and EoS Modelling for Compositional Thermal Simulation of Flow in Porous Media*, Springer International Publishing, 2019. <https://books.google.com.br/books?id=UTuIDwAAQBAJ>.
- [27] G.M. Kontogeorgis, G.K. Folas, *Thermodynamic Models for Industrial Applications: From Classical and Advanced Mixing Rules to Association Theories*, Wiley, 2009. https://books.google.com.br/books?id=kLFpSK_PmjIC.
- [28] M.-J. Huron, J. Vidal, New mixing rules in simple equations of state for representing vapour-liquid equilibria of strongly non-ideal mixtures, *Fluid Phase Equilib.* 3 (1979) 255–271. [https://doi.org/10.1016/0378-3812\(79\)80001-1](https://doi.org/10.1016/0378-3812(79)80001-1).
- [29] H. Renon, J.M. Prausnitz, Local compositions in thermodynamic excess functions for liquid mixtures, *AIChE J.* 14 (1968) 135–144. <https://doi.org/10.1002/aic.690140124>.
- [30] M.L. Michelsen, A modified Huron-Vidal mixing rule for cubic equations of state, *Fluid Phase Equilib.* 60 (1990) 213–219. [https://doi.org/10.1016/0378-3812\(90\)85053-D](https://doi.org/10.1016/0378-3812(90)85053-D).
- [31] K.S. Pedersen, M.L. Michelsen, A.O. Fredheim, Phase equilibrium calculations for unprocessed well streams containing hydrate inhibitors, *Fluid Phase Equilib.* 126 (1996) 13–28. [https://doi.org/10.1016/S0378-3812\(96\)03142-1](https://doi.org/10.1016/S0378-3812(96)03142-1).
- [32] G.M. Kontogeorgis, E.C. Voutsas, I. V. Yakoumis, D.P. Tassios, An equation of state for associating

- fluids, *Ind. Eng. Chem. Res.* 35 (1996) 4310–4318. <https://doi.org/10.1021/ie9600203>.
- [33] I. Tsivintzelis, G.M. Kontogeorgis, Modelling phase equilibria for acid gas mixtures using the CPA equation of state. Part VI. Multicomponent mixtures with glycols relevant to oil and gas and to liquid or supercritical CO₂ transport applications, *J. Chem. Thermodyn.* 93 (2016) 305–319. <https://doi.org/10.1016/J.JCT.2015.07.003>.
- [34] I. Tsivintzelis, G.M. Kontogeorgis, M.L. Michelsen, E.H. Stenby, Modeling phase equilibria for acid gas mixtures using the CPA equation of state. Part II: Binary mixtures with CO₂, *Fluid Phase Equilib.* 56 (2011) 2965–2982. <https://doi.org/10.1016/J.FLUID.2011.02.006>.
- [35] I. Tsivintzelis, S. Ali, G.M. Kontogeorgis, Modeling Phase Equilibria for Acid Gas Mixtures using the Cubic-Plus-Association Equation of State. 3. Applications Relevant to Liquid or Supercritical CO₂ Transport, *J. Chem. Eng. Data.* 59 (2014) 2955–2972. <https://doi.org/10.1021/je500090q>.
- [36] I. Tsivintzelis, S. Ali, G.M. Kontogeorgis, Modeling phase equilibria for acid gas mixtures using the CPA equation of state. Part IV. Applications to mixtures of CO₂ with alkanes, *Fluid Phase Equilib.* 397 (2015) 1–17. <https://doi.org/10.1016/J.FLUID.2015.03.034>.
- [37] M.B. Oliveira, L.A. Follegatti-Romero, M. Lanza, F.R.M. Batista, E.A.C. Batista, A.J.A. Meirelles, Low pressure vapor–liquid equilibria modeling of biodiesel related systems with the Cubic-Plus-Association (CPA) equation of state, *Fuel.* 133 (2014) 224–231. <https://doi.org/10.1016/J.FUEL.2014.05.016>.
- [38] I. Tsivintzelis, G.M. Kontogeorgis, Modelling phase equilibria for acid gas mixtures using the CPA equation of state. Part V: Multicomponent mixtures containing CO₂ and alcohols, *J. Supercrit. Fluids.* 104 (2015) 29–39. <https://doi.org/10.1016/j.supflu.2015.05.015>.
- [39] I. Tsivintzelis, G.M. Kontogeorgis, On the predictive capabilities of CPA for applications in the chemical industry: Multicomponent mixtures containing methyl-methacrylate, dimethyl-ether or acetic acid, *Chem. Eng. Res. Des.* 92 (2014) 2947–2969. <https://doi.org/10.1016/J.CHERD.2014.03.011>.
- [40] W. Xiong, X.-Q. Bian, Y.-B. Liu, Phase equilibrium modeling for methane solubility in aqueous sodium chloride solutions using an association equation of state, *Fluid Phase Equilib.* 506 (2020) 112416. <https://doi.org/10.1016/J.FLUID.2019.112416>.
- [41] A. Austegard, E. Solbraa, G. de Koeijer, M.J. Mølnvik, Thermodynamic models for calculating mutual solubilities in H₂O-CO₂-CH₄ mixtures, *Chem. Eng. Res. Des.* 84 (2006) 781–794. <https://doi.org/10.1205/cherd05023>.
- [42] K.S. Pedersen, J. Milter, C.P. Rasmussen, Mutual solubility of water and a reservoir fluid at high temperatures and pressures: Experimental and simulated data, *Fluid Phase Equilib.* 189 (2001) 85–97. [https://doi.org/10.1016/S0378-3812\(01\)00562-3](https://doi.org/10.1016/S0378-3812(01)00562-3).
- [43] G.M. Kontogeorgis, I. V. Yakoumis, H. Meijer, E. Hendriks, T. Moorwood, Multicomponent phase equilibrium calculations for water–methanol–alkane mixtures, *Fluid Phase Equilib.* 158–160 (1999) 201–209. [https://doi.org/10.1016/S0378-3812\(99\)00060-6](https://doi.org/10.1016/S0378-3812(99)00060-6).
- [44] K.V.M. Cavalcanti, L.M.L.A. Follegatti-Romero, I. Dalmolin, L.M.L.A. Follegatti-Romero, Liquid-

liquid equilibrium for (water + 5-hydroxymethylfurfural + 1-pentanol/1-hexanol/1-heptanol) systems at 298.15 K, *J. Chem. Thermodyn.* 138 (2019) 59–66. <https://doi.org/10.1016/J.JCT.2019.06.010>.

[45] L.A. Follegatti-Romero, M. Lanza, C.A.S. da Silva, E.A.C. Batista, A.J.A. Meirelles, Mutual Solubility of Pseudobinary Systems Containing Vegetable Oils and Anhydrous Ethanol from (298.15 to 333.15) K, *J. Chem. Eng. Data.* 55 (2010) 2750–2756. <https://doi.org/10.1021/je900983x>.

[46] O. Redlich, J.N.S. Kwong, On the Thermodynamics of Solutions. V. An Equation of State. Fugacities of Gaseous Solutions., *Chem. Rev.* 44 (1949) 233–244. <https://doi.org/10.1021/cr60137a013>.

[47] S.H. Huang, M. Radosz, Equation of state for small, large, polydisperse, and associating molecules, *Ind. Eng. Chem. Res.* 29 (1990) 2284–2294. <https://doi.org/10.1021/ie00107a014>.

[48] C.A. Perakis, E.C. Voutsas, K.G. Magoulas, D.P. Tassios, Thermodynamic Modeling of the Water + Acetic Acid + CO₂ System: The Importance of the Number of Association Sites of Water and of the Nonassociation Contribution for the CPA and SAFT-Type Models, *Ind. Eng. Chem. Res.* 46 (2007) 932–938. <https://doi.org/10.1021/ie0609416>.

[49] G.D. Pappa, C. Perakis, I.N. Tsimpanogiannis, E.C. Voutsas, Thermodynamic modeling of the vapor–liquid equilibrium of the CO₂/H₂O mixture, *Fluid Phase Equilib.* 284 (2009) 56–63. <https://doi.org/10.1016/J.FLUID.2009.06.011>.

[50] R.A. Cox, Acids and Bases. Solvent Effects on Acid–Base Strength. By Brian G. Cox., *Angew. Chemie Int. Ed.* 52 (2013) 7638. <https://doi.org/10.1002/anie.201304650>.

[51] L.R. Snyder, Classification off the Solvent Properties of Common Liquids, *J. Chromatogr. Sci.* 16 (1978) 223–234. <https://doi.org/10.1093/chromsci/16.6.223>.

[52] G.K. Folas, G.M. Kontogeorgis, M.L. Michelsen, E.H. Stenby, Application of the Cubic-Plus-Association (CPA) Equation of State to Complex Mixtures with Aromatic Hydrocarbons, *Ind. Eng. Chem. Res.* 45 (2006) 1527–1538. <https://doi.org/10.1021/ie050976q>.

[53] N. von Solms, M.L. Michelsen, G.M. Kontogeorgis, Applying Association Theories to Polar Fluids, *Ind. Eng. Chem. Res.* 43 (2004) 1803–1806. <https://doi.org/10.1021/ie034243m>.

[54] P.J. Linstrom, W.G. Mallard, The NIST Chemistry WebBook: A Chemical Data Resource on the Internet, *J. Chem. Eng. Data.* 46 (2001) 1059–1063. <https://doi.org/10.1021/je000236i>.

[55] I. Tsivintzelis, S. Ali, G.M. Kontogeorgis, Modeling systems relevant to the biodiesel production using the CPA equation of state, *Fluid Phase Equilib.* 430 (2016) 75–92. <https://doi.org/https://doi.org/10.1016/j.fluid.2016.09.018>.

[56] M.B. Oliveira, F.R. Varanda, I.M. Marrucho, A.J. Queimada, J.A.P. Coutinho, Prediction of Water Solubility in Biodiesel with the CPA Equation of State, *Ind. Eng. Chem. Res.* 47 (2008) 4278–4285. <https://doi.org/10.1021/ie800018x>.

[57] G.K. Folas, G.M. Kontogeorgis, M.L. Michelsen, E.H. Stenby, Application of the Cubic-Plus-Association Equation of State to Mixtures with Polar Chemicals and High Pressures, *Ind. Eng. Chem. Res.* 45 (2006) 1516–1526. <https://doi.org/10.1021/ie0509241>.

[58] A. Pourabadeh, A. Sanjari Fard, H. Jalaei Salmani, VLE and viscosity modeling of N-methyl-2-

pyrrolidone (NMP) + water (or 2-propanol or 2-butanol) mixtures by cubic-plus-association equation of state, *J. Mol. Liq.* 307 (2020) 112980. <https://doi.org/https://doi.org/10.1016/j.molliq.2020.112980>.

[59] J.A.P. Coutinho, P.M. Vlamos, G.M. Kontogeorgis, General Form of the Cross-Energy Parameter of Equations of State, *Ind. Eng. Chem. Res.* 39 (2000) 3076–3082. <https://doi.org/10.1021/ie990904x>.

[60] M.B. Oliveira, A.J.A.J. Queimada, G.M. Kontogeorgis, J.A.P.J.A.P. Coutinho, Evaluation of the CO₂ behavior in binary mixtures with alkanes, alcohols, acids and esters using the Cubic-Plus-Association Equation of State, *J. Supercrit. Fluids.* 55 (2011) 876–892. <https://doi.org/10.1016/j.supflu.2010.09.036>.

[61] P.W. Bell, A.J. Thote, Y. Park, R.B. Gupta, C.B. Roberts, Strong Lewis Acid–Lewis Base Interactions between Supercritical Carbon Dioxide and Carboxylic Acids: Effects on Self-association, *Ind. Eng. Chem. Res.* 42 (2003) 6280–6289. <https://doi.org/10.1021/ie030169w>.

[62] A. Kordikowski, A.P. Schenk, R.M. Van Nielen, C.J. Peters, Volume expansions and vapor-liquid equilibria of binary mixtures of a variety of polar solvents and certain near-critical solvents, *J. Supercrit. Fluids.* 8 (1995) 205–216. [https://doi.org/10.1016/0896-8446\(95\)90033-0](https://doi.org/10.1016/0896-8446(95)90033-0).

[63] M.L. Corazza, L.C. Filho, O.A.C. Antunes, C. Dariva, High Pressure Phase Equilibria of the Related Substances in the Limonene Oxidation in Supercritical CO₂, *J. Chem. Eng. Data.* 48 (2003) 354–358. <https://doi.org/10.1021/je020150k>.

[64] C.-Y. Day, C.J. Chang, C.-Y. Chen, Phase Equilibrium of Ethanol + CO₂ and Acetone + CO₂ at Elevated Pressures, *J. Chem. Eng. Data.* 41 (1996) 839–843. <https://doi.org/10.1021/je960049d>.

[65] C.J. Chang, K.-L. Chiu, C.-Y. Day, A new apparatus for the determination of P–x–y diagrams and Henry’s constants in high pressure alcohols with critical carbon dioxide, *J. Supercrit. Fluids.* 12 (1998) 223–237. [https://doi.org/10.1016/S0896-8446\(98\)00076-X](https://doi.org/10.1016/S0896-8446(98)00076-X).

[66] J. Chen, W. Wu, B. Han, L. Gao, T. Mu, Z. Liu, T. Jiang, J. Du, Phase Behavior, Densities, and Isothermal Compressibility of CO₂ + Pentane and CO₂ + Acetone Systems in Various Phase Regions, *J. Chem. Eng. Data.* 48 (2003) 1544–1548. <https://doi.org/10.1021/je034087q>.

[67] T. Adrian, G. Maurer, Solubility of Carbon Dioxide in Acetone and Propionic Acid at Temperatures between 298 K and 333 K, *J. Chem. Eng. Data.* 42 (1997) 668–672. <https://doi.org/10.1021/je970011g>.

[68] M.J. Lazzaroni, D. Bush, J.S. Brown, C.A. Eckert, High-Pressure Vapor–Liquid Equilibria of Some Carbon Dioxide + Organic Binary Systems, *J. Chem. Eng. Data.* 50 (2005) 60–65. <https://doi.org/10.1021/je0498560>.

[69] J. Im, W. Bae, J. Lee, H. Kim, Vapor–Liquid Equilibria of the Binary Carbon Dioxide–Tetrahydrofuran Mixture System, *J. Chem. Eng. Data.* 49 (2004) 35–37. <https://doi.org/10.1021/je0202228>.

[70] Ž. Knez, M. Škerget, L. Ilić, C. Lütge, Vapor–liquid equilibrium of binary CO₂–organic solvent systems (ethanol, tetrahydrofuran, ortho-xylene, meta-xylene, para-xylene), *J. Supercrit. Fluids.* 43 (2008) 383–389. <https://doi.org/10.1016/J.SUPFLU.2007.07.020>.

[71] T. Aida, T. Aizawa, M. Kanakubo, H. Nanjo, Dependence of volume expansion on alkyl chain length and the existence of branched methyl group of CO₂-expanded ketone systems at 40 °C, *J. Supercrit. Fluids.* 55 (2010) 71–76. <https://doi.org/10.1016/J.SUPFLU.2010.05.025>.

- 710 [72] X. Gui, Z. Tang, W. Fei, Solubility of CO₂ in Alcohols, Glycols, Ethers, and Ketones at High Pressures
711 from (288.15 to 318.15) K, J. Chem. Eng. Data. 56 (2011) 2420–2429.
712 <https://doi.org/10.1021/je101344v>.
- 713 [73] G. Anişescu, I. Găinar, R. Vilcu, Solubility of carbon dioxide in some solvents containing ketone group
714 at high pressures, Rev. Roum. Chim. (1996).
- 715 [74] C. Duran-Valencia, A. Valtz, L.A. Galicia-Luna, D. Richon, Isothermal Vapor–Liquid Equilibria of the
716 Carbon Dioxide (CO₂)–N,N-Dimethylformamide (DMF) System at Temperatures from 293.95 K to
717 338.05 K and Pressures up to 12 MPa, J. Chem. Eng. Data. 46 (2001) 1589–1592.
718 <https://doi.org/10.1021/je010055w>.
- 719 [75] H.-Y. Chiu, R.-F. Jung, M.-J. Lee, H.-M. Lin, Vapor–liquid phase equilibrium behavior of mixtures
720 containing supercritical carbon dioxide near critical region, J. Supercrit. Fluids. 44 (2008) 273–278.
721 <https://doi.org/10.1016/J.SUPFLU.2007.09.026>.
- 722 [76] A. Vega Gonzalez, R. Tufeu, P. Subra, High-Pressure Vapor–Liquid Equilibrium for the Binary Systems
723 Carbon Dioxide + Dimethyl Sulfoxide and Carbon Dioxide + Dichloromethane, J. Chem. Eng. Data. 47
724 (2002) 492–495. <https://doi.org/10.1021/je010202q>.
- 725 [77] M.S. Shin, J.H. Lee, H. Kim, Phase behavior of the poly(vinyl
726 pyrrolidone) + dichloromethane + supercritical carbon dioxide system, Fluid Phase Equilib. 272 (2008)
727 42–46. <https://doi.org/10.1016/J.FLUID.2008.07.016>.
- 728 [78] S. Tian, Y. Hou, W. Wu, S. Ren, K. Pang, Physical Properties of 1-Butyl-3-methylimidazolium
729 Tetrafluoroborate/N-Methyl-2-pyrrolidone Mixtures and the Solubility of CO₂ in the System at Elevated
730 Pressures, J. Chem. Eng. Data. 57 (2012) 756–763. <https://doi.org/10.1021/je200886j>.
- 731 [79] F. MURRIETA-GUEVARA, A. TREJO RODRIGUEZ, Solubility of carbon dioxide, hydrogen sulfide,
732 and methane in pure and mixed solvents, J. Chem. Eng. Data. 29 (1984) 456–460.
- 733 [80] C.-W. Lee, C.-Y. Jung, H.-S. Byun, High Pressure Phase Behavior of Carbon Dioxide + 1-Methyl-2-
734 pyrrolidinone and Carbon Dioxide + 1-Ethyl-2-pyrrolidinone Systems, J. Chem. Eng. Data. 49 (2004)
735 53–57. <https://doi.org/10.1021/je0301545>.
- 736